

Chapter-4

Results

4. Results:

4.1 Blank experiments

The blank activity of the micro-flow reactor was checked in 2 different experiments. The first experiment was done to test if there is any reaction on the reactor cup, since during reaction experiments the reactor cup temperature reaches ~ 670 K and also since the surface area of the reactor cap is much larger than the surface area of the single crystal sample. The reactor cap was heated up to ~ 730 K the reactants were admitted to the reactor and the activity was followed for more than 1 hour. No styrene conversion or other byproducts were detected.

A second blank experiment was done by measuring the styrene conversion rate on a sample incidentally contaminated by SiO_2 . The conversion rate was below $\sim 0.1 \times 10^{15} \text{ cm}^{-2} \text{ s}^{-1}$, which is the detection limit of our GC. This represents the upper limit of the blind activity of the micro-flow reactor.

4.2 Unpromoted model catalysts

4.2.1 Dehydrogenation reaction on $\alpha\text{-Fe}_2\text{O}_3$ (0001) and Fe_3O_4 (111) model catalysts in presence of steam.

As Fig. (4.1) shows that the reaction on the clean unpromoted $\alpha\text{-Fe}_2\text{O}_3$ (0001) model catalyst starts with a high St conversion rate of $\sim 4 \times 10^{15} \text{ molecules. s}^{-1}.\text{cm}^{-2}$, then this rate decreases with time on stream until it reaches a steady state after about 70 min with a rate of $\sim 0.5 \times 10^{15} \text{ molecules. s}^{-1}.\text{cm}^{-2}$. Post reaction characterization with AES showed that there is a significant amount of graphitic carbon deposits on the catalyst surface ($\mathbf{I}_C/\mathbf{I}_{\text{Fe}}$ is ~ 3.4). After removal by performing a few TPO cycles, LEED showed that the surface exhibits the LEED pattern of Fe_3O_4 (C in table(1)).

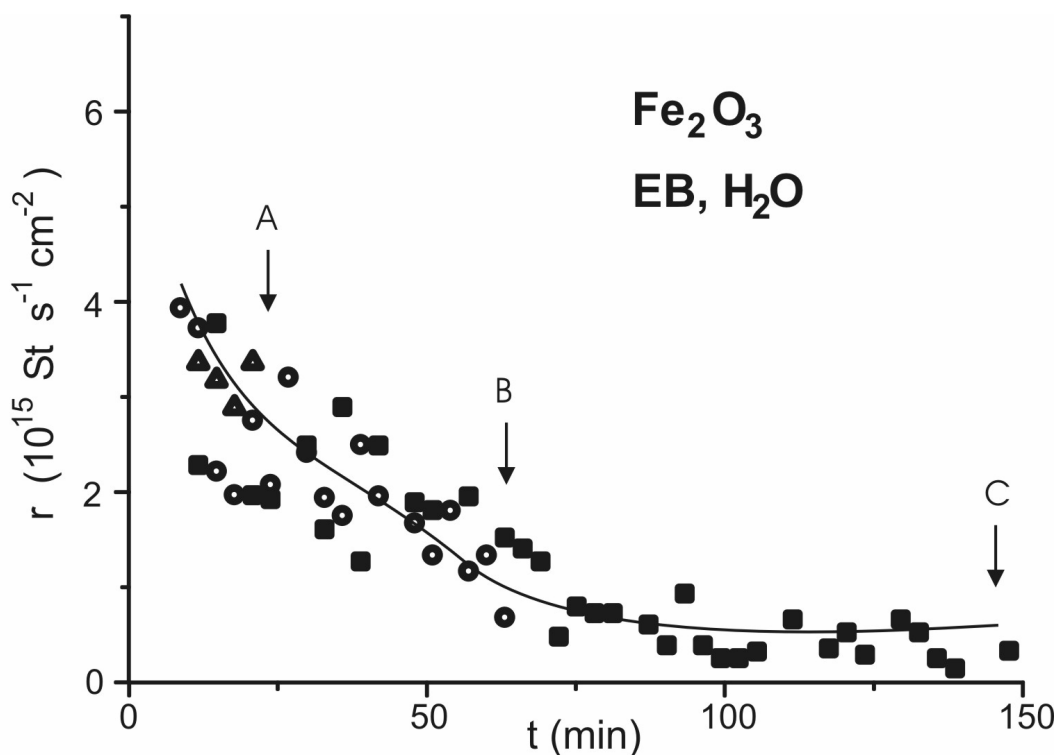
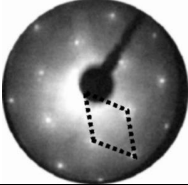
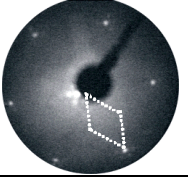
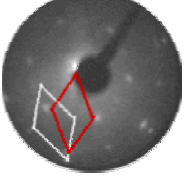
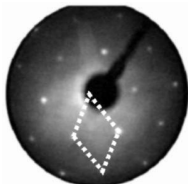


Fig. (4.1). Time dependence of the St yield rate at 870 K, normal conditions, EB and H₂O in the feed, over α -Fe₂O₃(0001). The labels A-C give the positions where sample characterization was performed (see table (4.1)).

A detailed investigation of this deactivation behavior on the catalyst was done by repeating and interrupting the reaction on freshly prepared samples after different times from starting the reaction Fig. (4.1). The results showed that in the high yield rate region at point **A** there is a small amount of carbon deposited I_C/I_{Fe} is ~ 1 and there is a small decrease in the I_O/I_{Fe} ratio. After 1 TPO cycle, LEED showed the film is still Fe₂O₃ but some changes on the surface (it is rougher) since the LEED spots became much more diffused. At point **B** AES showed that the amount of carbon deposits on the surface has increased. LEED showed that the Fe₂O₃ is now partially reduced to Fe₃O₄ since it exhibits a superposition LEED pattern of these both phases (table (4.1)).

Table 4.1. LEED patterns and intensity ratios of the main Auger peaks of carbon, oxygen and iron before and after reaction for the unpromoted Fe₂O₃ model catalysts.

Treatment	LEED pattern	Phase from LEED	Auger intensity ratios		Label in Fig. 4.1
			I _C /I _{Fe}	I _O /I _{Fe}	
Fe ₂ O ₃ before reaction		Fe ₂ O ₃	0	3.5	-
After reaction with EB H ₂ O		after 1 TPO cycle: Fe ₂ O ₃	1.1	3.2	A
		after 3 TPO cycles: Fe ₂ O ₃ and Fe ₃ O ₄	3.6	4.0	B
		after 1 TPO cycle: Fe ₃ O ₄	3.4	3.8	C

After reaction, one Fe₂O₃ sample was also transferred ex-situ for characterization with STM. Comparing the STM images in Fig.(4.2) of the catalyst surface before and after reaction shows clearly that, there is an increase in the surface roughness after reaction and that the surface is covered by carbon deposits. But it is not possible from STM measurements to see if the surface is completely covered by a closed layer of carbon deposits or if these carbon deposits are in form of islands on the surface.

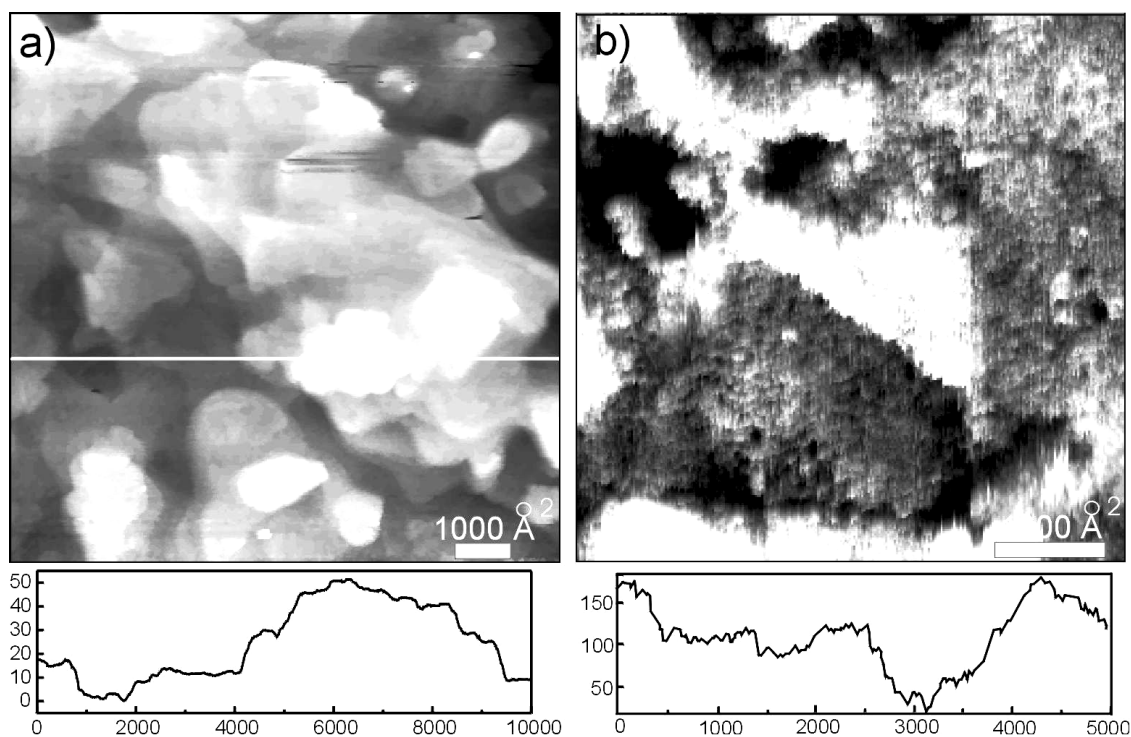


Fig. (4.2). STM images of an unpromoted Fe_2O_3 model catalyst surface a) before reaction, b) after 3 hours reaction at 870 K ($\text{EB}:\text{H}_2\text{O} = 1:10$), with the height profile of each image shown below.

The deactivated Fe_2O_3 sample after reaction (C in Fig. (4.1)) was brought back to the reactor after characterization with AES in the TDS chamber (without TPO cycles), the reaction was continued on the sample. The sample showed the final activity of $\sim 0.5 \times 10^{15}$ molecules $\text{cm}^{-2} \text{s}^{-1}$, which was observed on the deactivated the sample before.

For comparison with Fe_2O_3 the reaction was done on a clean Fe_3O_4 (Fig (4.3)). It showed a lower starting St conversion rate of $\sim 2 \times 10^{15}$ molecules $\text{s}^{-1}\text{cm}^{-2}$, then deactivates after ~ 45 min from reaction, to the same steady state rate as seen on the Fe_2O_3 . Post reaction characterization with AES showed that the surface was covered by carbon deposits ($\mathbf{I}_\text{C}/\mathbf{I}_\text{Fe}$ is ~ 5.0). After TPO cycles the surface still exhibits the Fe_3O_4 -

(111) LEED pattern but the intensity of the spots is wider which indicates the increase in surface roughness during reaction (**E** in table (4.2)).

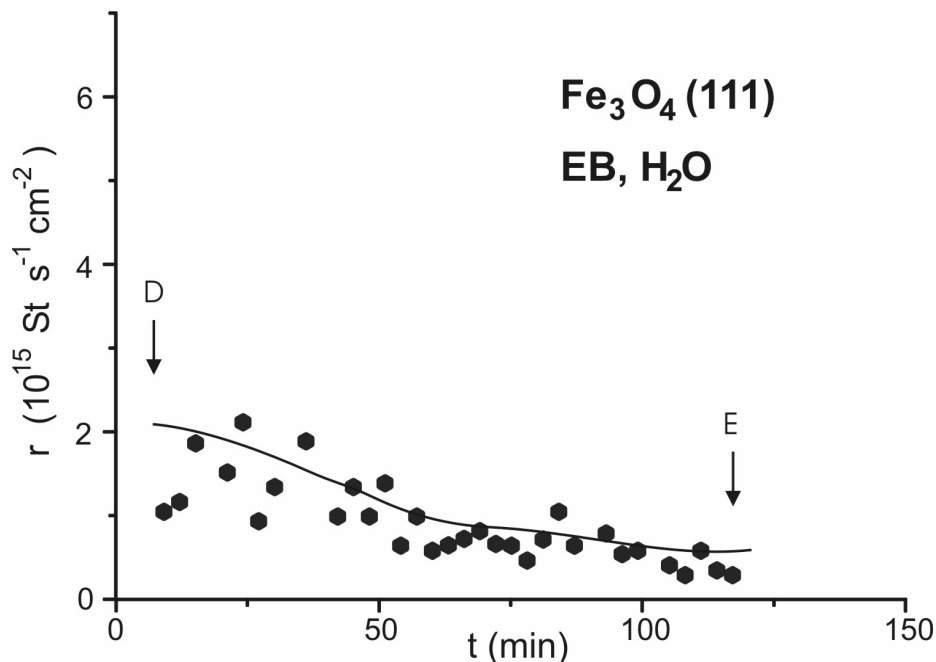


Fig. (4.3). Time dependence of the St conversion rate at 870 K, normal conditions, EB and H₂O in the feed, over Fe₃O₄. The label D and E give the position where sample characterization was performed (see table 4.2).

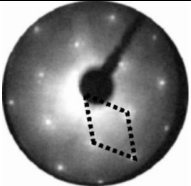
Table 4.2 .LEED patterns and intensity ratios of the main Auger peaks of carbon, oxygen and iron before and after different treatments for the unpromoted Fe₃O₄ model catalysts

Treatment	LEED pattern	Phase from LEED	Auger intensity ratios		Label Fig. 4.3
			I _C /I _{Fe}	I _O /I _{Fe}	
Fe ₃ O ₄ Before reaction		Fe ₃ O ₄	0.0	2.9	D
Fe ₃ O ₄ After reaction with EB and H ₂ O		after 4 TPO cycle: Fe ₃ O ₄ , disordered	5.0	3.5	E

4.2.2 Dehydrogenation reaction on α -Fe₂O₃ (0001) model catalyst without steam.

In order to study the role of water in the dehydrogenation reaction, reaction experiments were done on the unpromoted α -Fe₂O₃ (0001) model catalyst without steam by introducing 20 ml of He alone with the EB in order to maintain the total flow constant. Fig.(4.4) shows that the St conversion exhibits the same high starting conversion rate $\sim 5 \times 10^{15}$ molecules s⁻¹ cm⁻², like the reaction with steam, then deactivates to the same steady state conversion rate like in reaction with steam. AES measurements after reaction (G in table (4.3)) showed that the surface was covered only with carbon deposits and the carbon layer was quit thick that even after more than 10 cycles of TPO experiments only carbon is still seen on the surface as shown in Fig. (4.5). The reaction was repeated and interrupted after ~ 50 min (F in Fig.(4.4)), the AES showed that the $I_{\text{O}}/I_{\text{Fe}}$ ratio has decreased quite strongly to 2.0 and there is a big amount of carbon deposits as seen from AES (F in table (4.3)). After 5 TPO cycles no LEED pattern of iron oxide could be seen which indicates that the iron oxide phase has been strongly reduced almost to metallic iron Fe⁰.

Table 4.3. LEED patterns and intensity ratios of the main Auger peaks of carbon, oxygen and iron before and after reaction without water for the unpromoted Fe₂O₃ model catalysts.

Treatment	LEED pattern	Phase from LEED	Auger intensity ratios		Label in Fig. 4.4
			I _C /I _{Fe}	I _O /I _{Fe}	
Fe ₂ O ₃ before reaction		Fe ₂ O ₃	0	3.5	-
After reaction with EB	no pattern		5.3	2.0	F
			∞	-	G

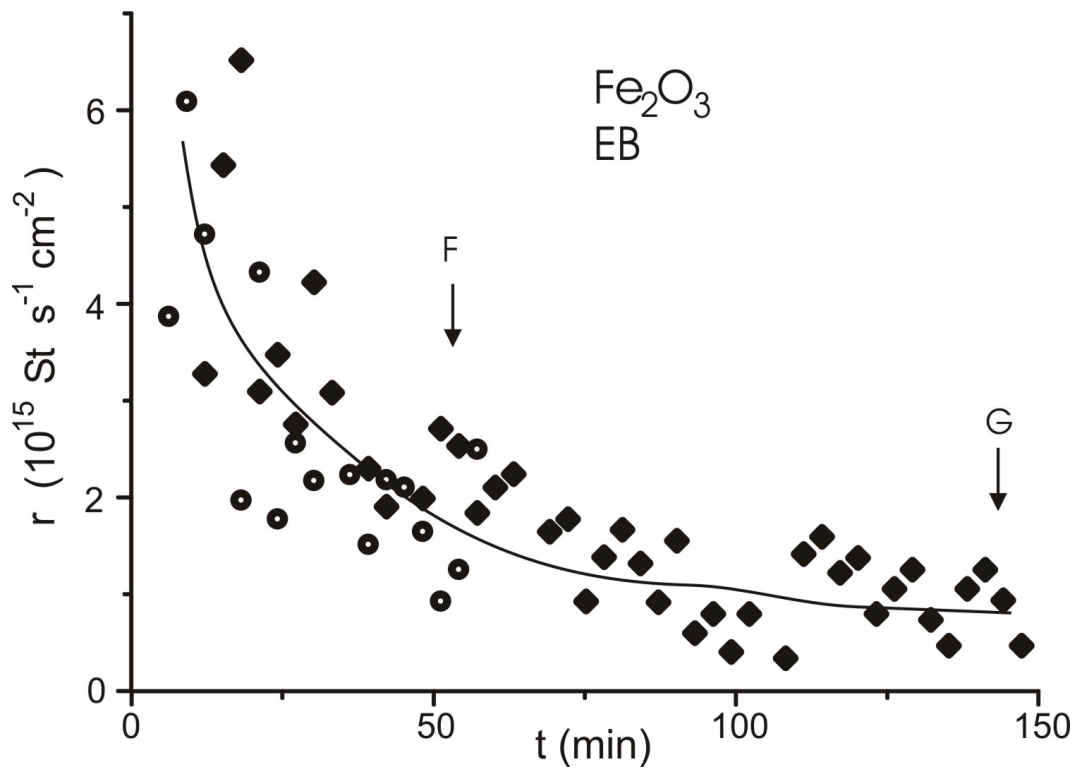


Fig. (4.4). Time dependence of the St conversion rate at 870 K, normal conditions, EB and He in the feed, over Fe_2O_3 . The label F and G give the position where sample characterization was performed (see table 4.3).

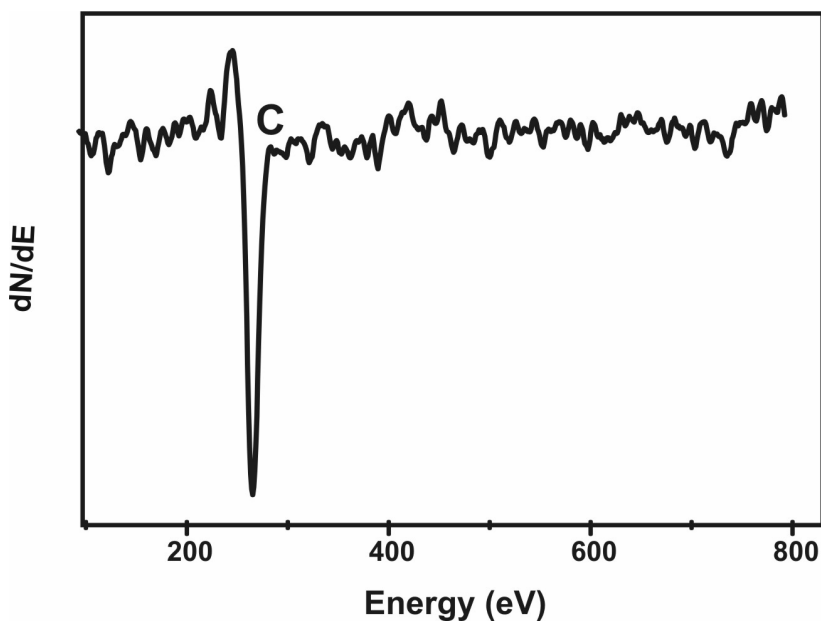


Fig. (4.5). AES spectrum of Fe_2O_3 model catalyst after reaction at 870 K, EB and He but no water in the feed. Only carbon signal at 270 eV is seen.

4.2.3 Dehydrogenation reaction on α - Fe_2O_3 (0001) model catalyst in presence of steam and oxygen.

The influence of dosing some oxygen in the feed on the reaction and deactivation behavior was studied. We have used here a mixture of 20 % oxygen in helium for dosing oxygen. The standard ratio of EB to oxygen (O_2) was $\sim 2:1$ (oxidative conditions, table 3.1). Fig (4.6) shows that by admitting small amount of oxygen in the feed mixture, the high initial St conversion rate $\sim 6 \times 10^{15}$ molecules. $\text{s}^{-1}.\text{cm}^{-2}$ decrease only slightly with time. AES measurement after the experiment (at H) showed that the surface is almost free of carbon $I_{\text{C}}/I_{\text{Fe}} = 0.8$ and the $I_{\text{O}}/I_{\text{Fe}}$ ratio is not changed during reaction. LEED after 1 TPO cycle showed that the film is still exhibits the α - Fe_2O_3 (0001) pattern but the surface is believed to be more rough since the background is high and the spots are broadened (H in table (4.4)).

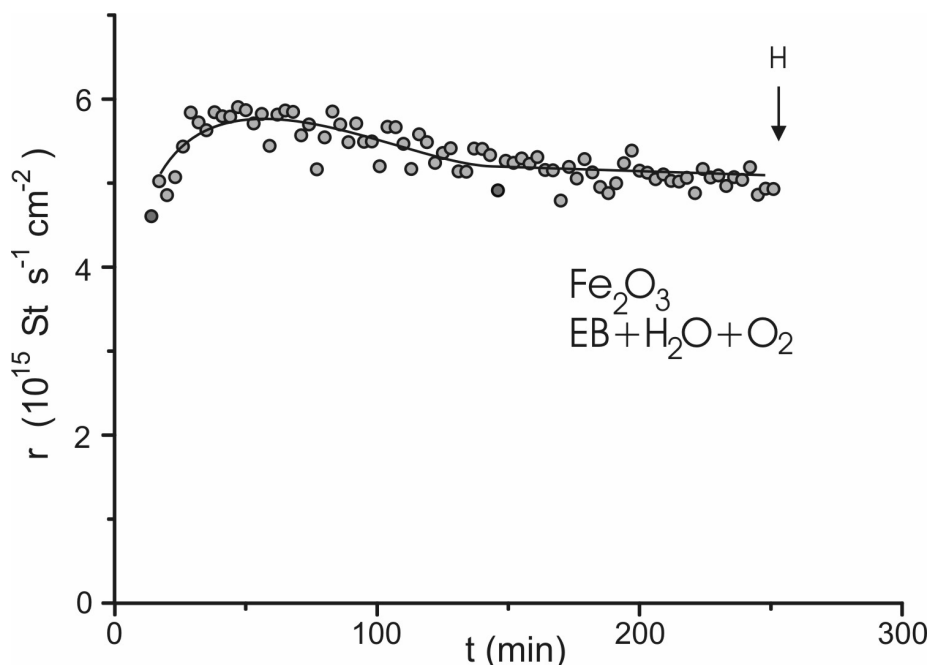
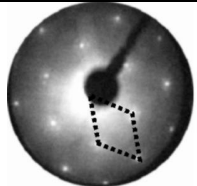
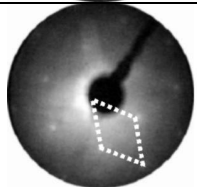


Fig. (4.6). Time dependence of the St conversion rate at 870 K, oxidative conditions, EB, H_2O and O_2 in the feed, over Fe_2O_3 . The label H gives the position where sample characterization was performed (see table 4.4).

Table 4.4. LEED patterns and intensity ratios of the main Auger peaks of carbon, oxygen and iron before and after reaction with EB, water and oxygen in the feed for the unpromoted Fe₂O₃ model catalysts.

Treatment	LEED pattern	Phase from LEED	Auger intensity ratios		Label Fig.4.6
			I _C /I _{Fe}	I _O /I _{Fe}	
Fe ₂ O ₃ before reaction		Fe ₂ O ₃	0	3.5	-
Reaction with EB H ₂ O O ₂		after 1 TPO cycle: Fe ₂ O ₃ , disordered	0.8	3.4	H

4.2.5 Dehydrogenation reaction on α -Fe₂O₃ (0001) model catalyst in presence of steam and oxygen, effect of oxygen concentration on the activity.

In order to determine the optimal concentration of oxygen needed to stabilize the high styrene conversion rate, the effect of decreasing the EB to oxygen molar ratio was studied. The oxygen ratio was decreased stepwise after ~ 50 minutes. Fig. (4.8) shows that decreasing the EB: O₂ ratio to 1:0.3 and to 1: 0.13 leads to a deactivation and a decrease in the steady state St conversion rate. The conversion rate can be regained after increasing the EB: O₂ ratio again as shown in detail in Fig. (4.7a). The relationship between the steady state rate taken from Fig. (4.7a) and EB:O₂ molar ratio is shown in Fig. (4.7b). This shows that the EB:O₂ ratio (1:0.5) is the optimal. This agrees quit well with an estimation we have made which is presented in the discussion in chapter 5.

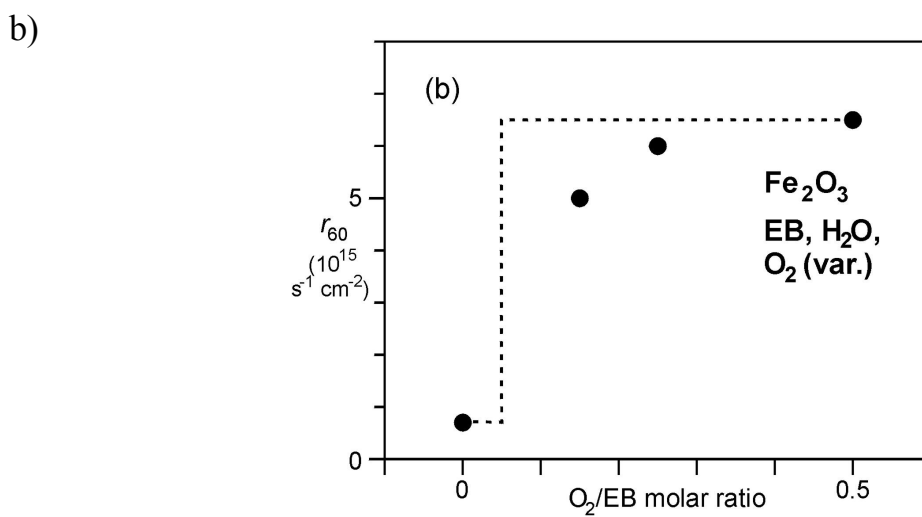
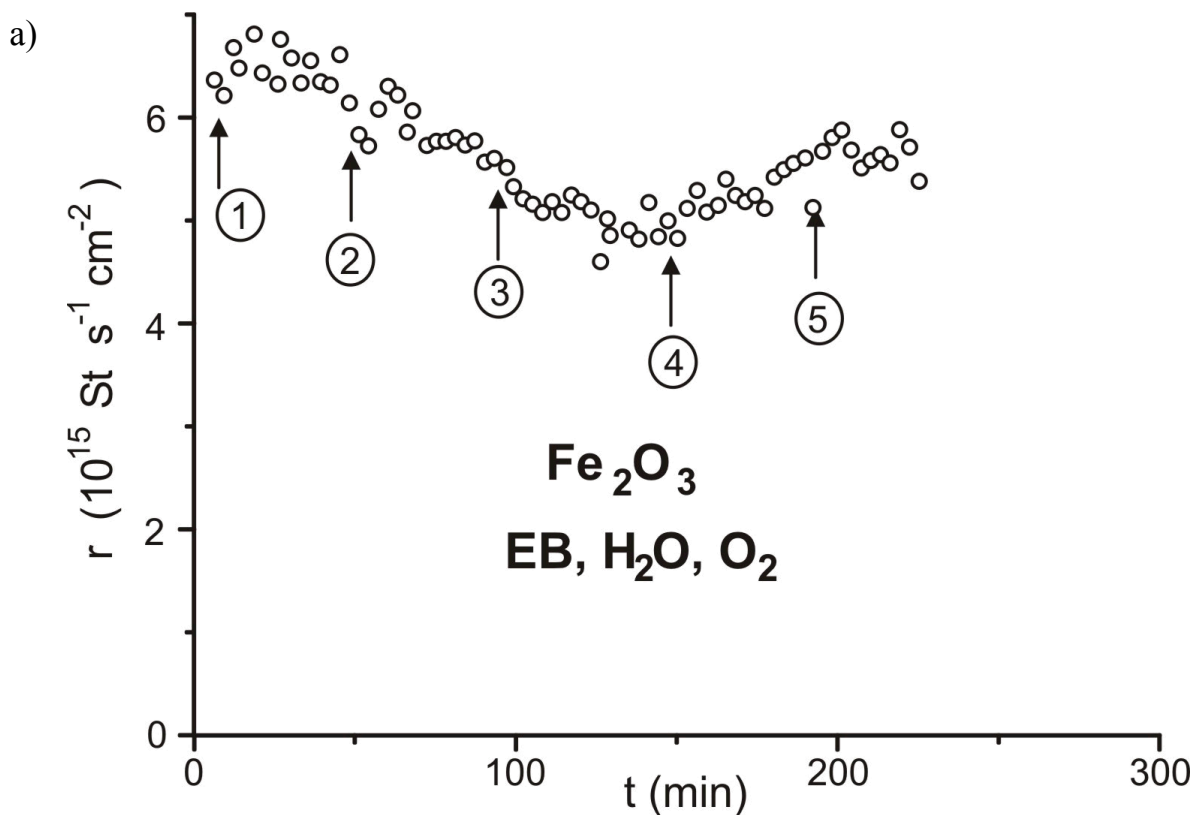


Fig. (4.7). a) Conversion dependence of the St conversion rate at 870 K, oxidative conditions, EB, H_2O and O_2 in the feed, over Fe_2O_3 on EB/ O_2 molar ratio which is changed at the position labeled by numbers (1) 1:0.5, (2) 1:0.3, (3) 1:0.13 and (4) 1:0.3. (5) 1:0.5 b) Dependence of the steady state rate after 50 reaction at constant EB: O_2 molar ratio (r_{50}). The dotted line is the estimated O_2 /EB molar ratio which is theoretically needed to stabilize the high initial St conversion.

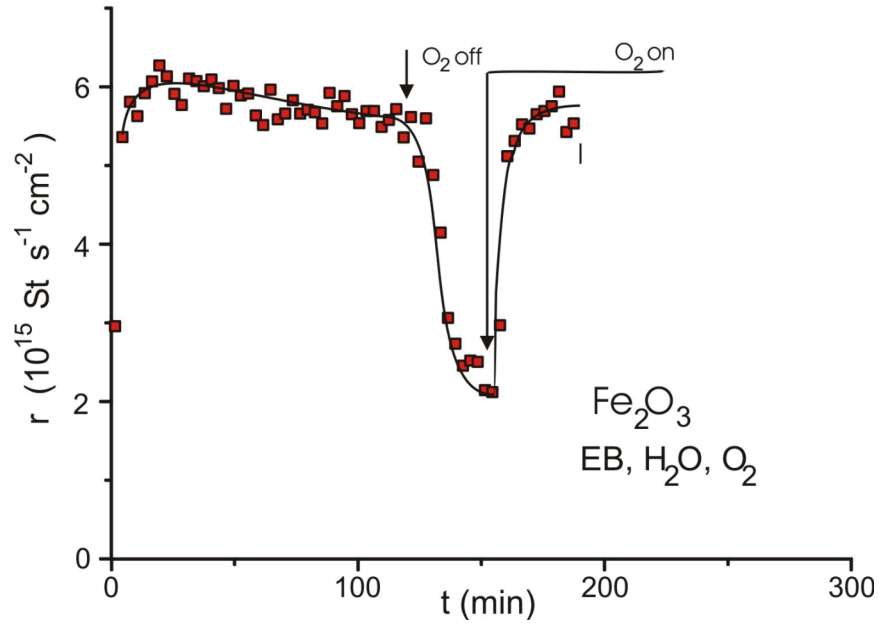
4.2.4 Dehydrogenation reaction on α -Fe₂O₃ (0001) model catalyst in presence of steam and oxygen. Oxygen on and off experiments.

The response of the conversion rate on the oxygen content in the feed is studied in on-off experiments. Fig. (4.8a) shows that within 2 hrs of reaction in presence of oxygen there is a slightly decrease of the conversion rate but after switching off the oxygen the deactivation is fast. In fact it is faster than when we start with the clean surface without oxygen (Fig. 4.1). After 30 min of switching the oxygen off it was switched on again. Within ~ 20 minutes the initial activity is regenerated. Post reaction characterization with AES showed that at point I in Fig.(4.8a) there is a small amount of carbon ($I_C/I_{Fe}=1.1$) and almost no change in the ($I_O/I_{Fe}=3.2$). After 1 TPO cycle the film shows the LEED pattern of Fe₂O₃ but the surface is rougher due to the high background in the LEED pattern I in table (4.5).

The reaction was repeated as shown in Fig. (4.8b). After ~ 4 hours reaction in the presence of oxygen in the feed, oxygen switch-off and -on were repeated twice. The deactivation and reactivation behavior of the catalyst is reproducible. 30 minutes after switching the oxygen off (**J** in Fig. (4.7b)), the reaction was interrupted and the sample transferred back to the UHV chamber for post-reaction characterization. AES shows that there are more carbon deposits on the surface ($I_C/I_{Fe}= 4.0$) and after 3 cycles of TPO, LEED shows mainly The Fe₃O₄ pattern but also with weak spots from the Fe₂O₃ . The surface is quite rough as concluded from the high background of the LEED image. Comparison of the deactivation rate with that on a fresh Fe₂O₃ model catalyst without oxygen in the feed (inserted low curve in Fig (4.8a) for comparison) shows that it is faster, this could be due to the increase of the roughness i.e disorder of the catalyst

surface as a result of recrystallization during reaction, this leads to an increase in the exchange between the solid and gas phase.

a)



b)

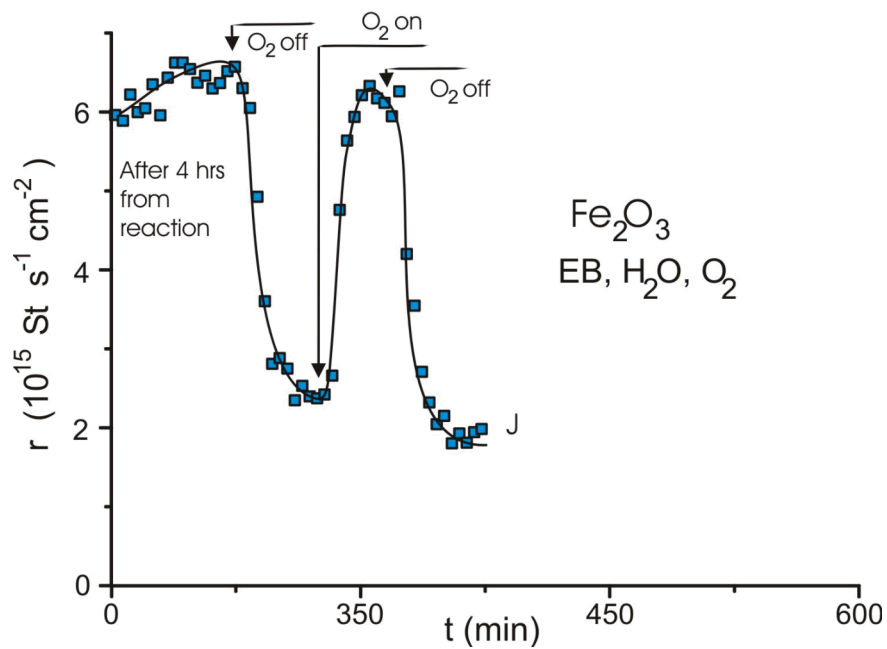
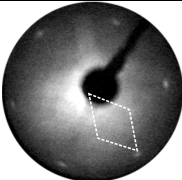
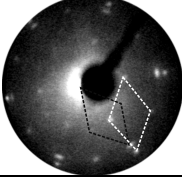


Fig. (4.8). Deactivation of the St conversion rate at 870 K, normal conditions, EB, H₂O and O₂ in the feed, over Fe₂O₃ after switching O₂ on and off a)and b). The label I and J give the position where sample characterization was performed (see table (4.5)).

Table 4.5. LEED patterns and intensity ratios of the main Auger peaks of carbon, oxygen and iron, before and after reaction with water and switching oxygen on and off in the feed, for the unpromoted Fe₂O₃ model catalysts.

Treatment	LEED pattern	Phase from LEED	Auger intensity ratios		Label in Fig.4.8
			I _C /I _{Fe}	I _O /I _{Fe}	
Reaction with EB, H ₂ O O ₂ on & off Fig. 4.7a		after 1 TPO cycle: Fe ₂ O ₃ , disordered	0.7	3.4	I
Reaction with EB, H ₂ O O ₂ on & off Fig. 4.7b		after 3 TPO cycle: Fe ₂ O ₃ + Fe ₃ O ₄	4.0	3.3	J

4.2.6 Dehydrogenation reaction on α -Fe₂O₃ (0001) model catalyst in presence of steam and oxygen at different temperatures.

Fig. (4.9) shows the dependence of the conversion rate to St over unpromoted Fe₂O₃ model catalyst in the presence of water and oxygen on the reaction temperature. The Figure shows quite clear the proportionality dependence of the conversion rate on the reaction temperature reflecting the endothermicity of the reaction, which agrees quite well with the literature [2]. Oxygen was added in these experiments in order to keep the catalyst surface clean and prevent deactivation during reaction, which allows the evaluation of the activation energy of almost the clean active surface. From this measurement an estimation of the activation energy will be calculated using the Arrhenius equation and shown in detail in the discussion chapter 5.

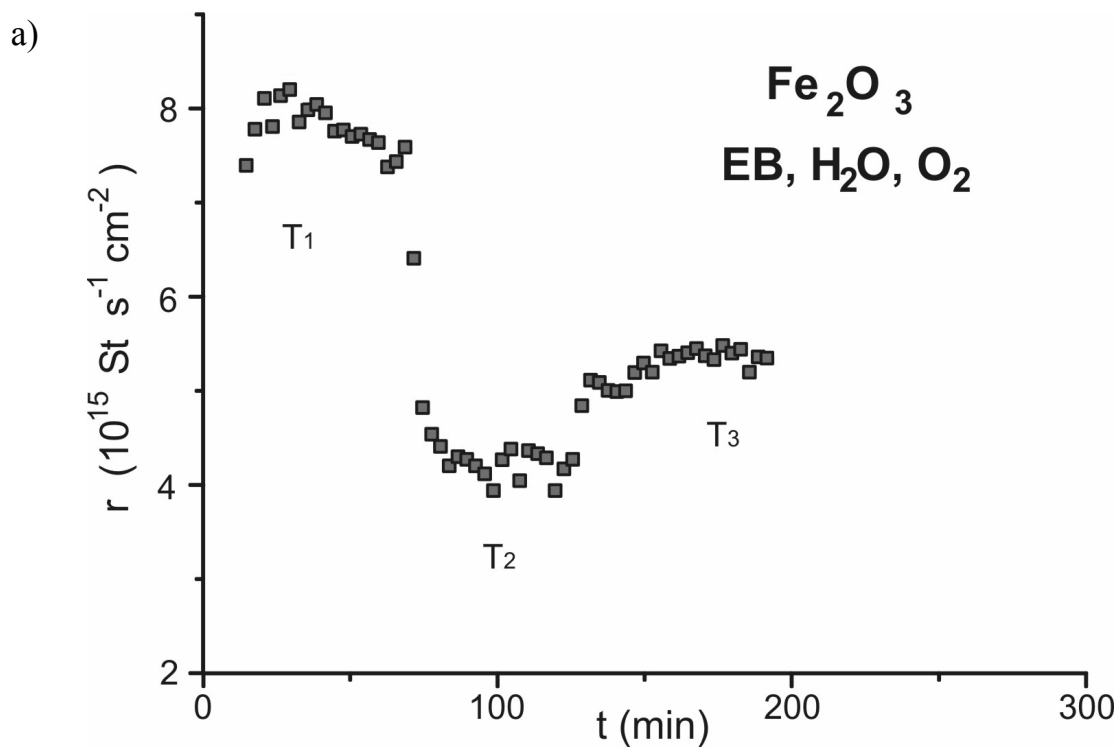


Fig. (4.9). The dependence of the St conversion rate at, normal conditions, EB, H₂O and O₂ in the feed, over Fe₂O₃ at reaction temperature T_1 (894 K), T_2 (850 K) and T_3 (870 k).

4.3 Promoted iron oxide (KFe_xO_y) model catalysts

4.3.1 Dehydrogenation reaction on KFe_xO_y model catalyst in presence of steam and the effect of potassium content.

Fig (4.10) shows the St conversion rate on the potassium promoted catalyst ($I_{\text{K}}/I_{\text{Fe}} = 2.2$). The catalyst starts with a high conversion rate of $\sim 4 \times 10^{15}$ molecules $\text{s}^{-1} \text{cm}^{-2}$ then deactivates much slower compared to the reaction on the unpromoted catalyst with steam. After ~ 4 hrs the promoted catalyst still exhibits a conversion rate of $\sim 2 \times 10^{15}$ molecules $\text{s}^{-1} \text{cm}^{-2}$ which is higher than on unpromoted catalyst with steam. After reaction there was an increase in the carbon deposits on the catalyst surface as AES showed ($I_{\text{C}}/I_{\text{Fe}} = 2.0$) which however, is less than in case of the reaction on unpromoted catalyst with steam. There is also no strong loss in the potassium content during the reaction (1 in table (4.6)).

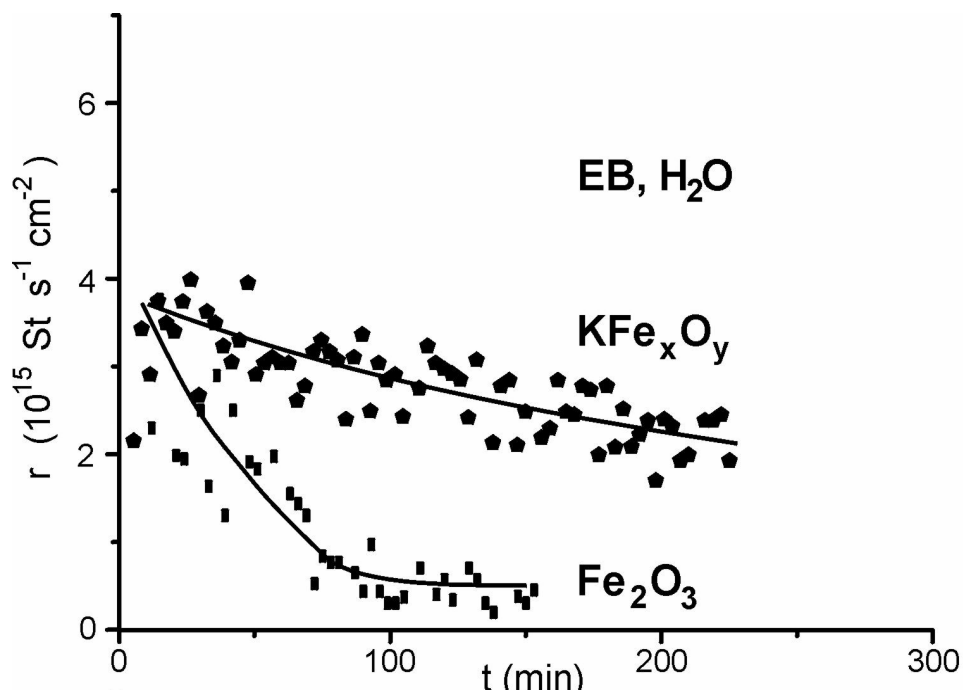


Figure 4.10. Time dependence of the St conversion rate at 870 K, normal conditions, EB and H_2O in the feed, over KFe_xO_y with a ($I_{\text{K}}/I_{\text{Fe}}=2.2$). The lower curve shows the St conversion rate over unpromoted Fe_2O_3 .

In order to study the influence of the potassium content on the catalyst behavior, the reaction was performed at first on a promoted catalyst with a low potassium content ($I_K/I_{Fe} = 0.9$) Fig. 4.11a. The catalyst has a higher starting conversion rate of $\sim 5 \times 10^{15}$ molecules $s^{-1}cm^{-2}$, but a faster deactivation and a lower final rate when compared to the reaction on the promoted catalyst in Fig(4.10). Comparing the AES measurements (1 and 2 in table (2)) on both model catalysts ($I_K/I_{Fe} = 2.2$ and 0.9) and ($I_K/I_{Fe} = 1.9$ and 0.7) before and after the reaction, respectively we see that there is a moderate loss in the potassium content during the reaction, There is also an increase in the carbon deposits on the catalyst surface see ($I_C/I_{Fe} = 2.0$ and 3.0) for cases 1 and 2 in table (4.6)).

Secondly the reaction was done over a promoted catalyst with a higher potassium content ($I_K/I_{Fe} = 4.2$). In order to obtain this high potassium content the sample was only annealed in oxygen at 870 K after potassium deposition. Under these conditions a $KFeO_2$ thin film is present on the catalyst surface as explained in (2.2.2 chapter 2). Fig. (4.11b) shows that it has a very low starting St conversion rate of $\sim 2 \times 10^{15}$ molecules $s^{-1}cm^{-2}$, but deactivation is considerably slower compared to Fig. (4.10). Post-reaction characterization with AES shows only little coke ($I_C/I_{Fe} = 1.1$) and only a moderate loss of potassium case 3 in table (4.6). This indicates clearly the effect of potassium content on the activity and deactivation of the promoted catalyst, high potassium content lead to low initial activity but low rate of deactivation and vice versa. This also shows clearly that $KFeO_2$ is not the active phase for this reaction .

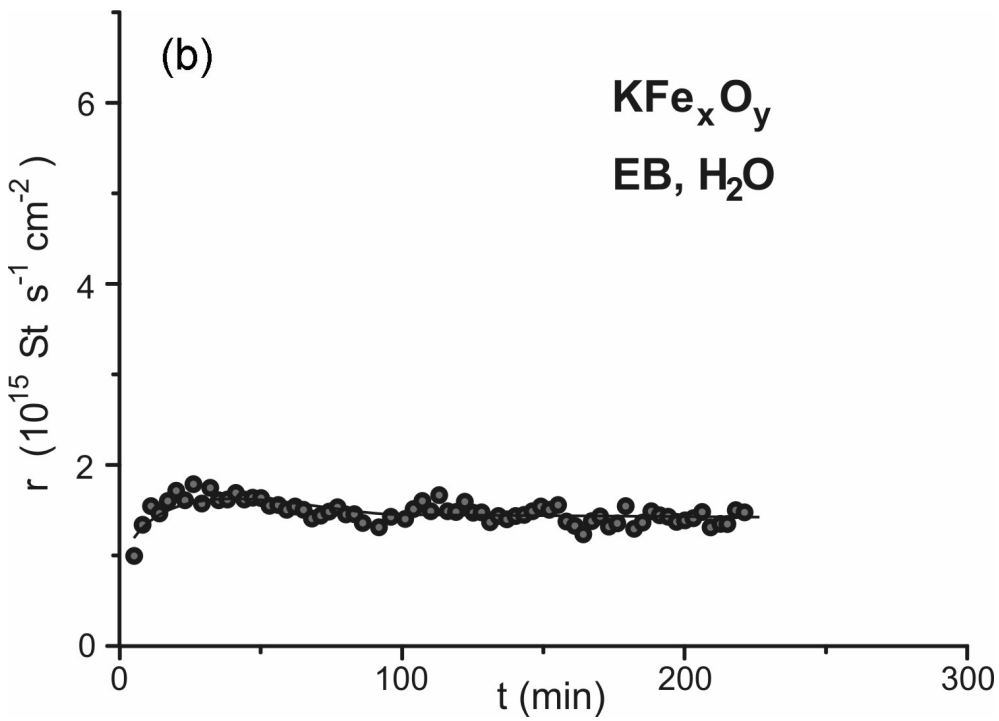
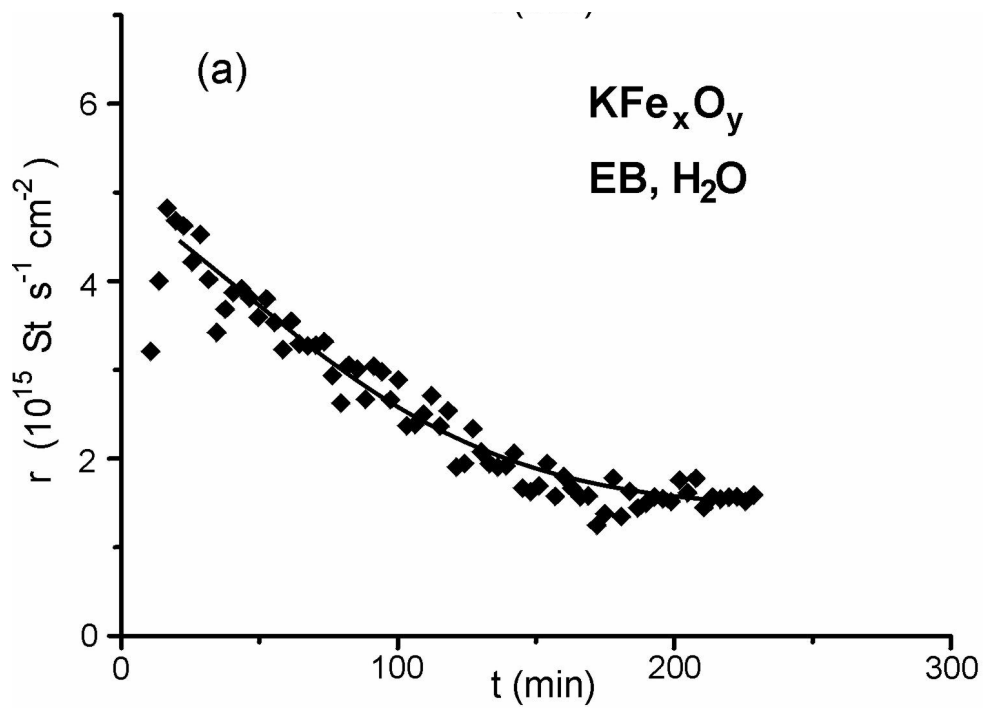
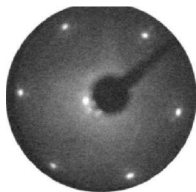
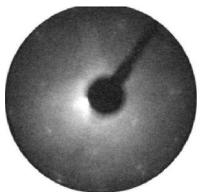
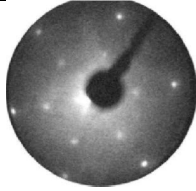
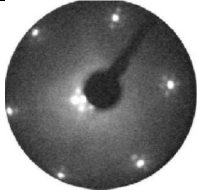


Fig. (4.11). Time dependence of the St conversion rate at 870 K, normal conditions, EB and H_2O in the feed, over KFe_xO_y , with a) ($I_K/I_{Fe} = 0.9$), b) ($I_K/I_{Fe} = 4.2$).

Table 4.6. LEED patterns and intensity ratios of the main Auger peaks of carbon, oxygen, potassium and iron before and after reaction with EB and H₂O in the feed for the promoted KFe_xO_y model catalysts with different K-loading.

KFe _x O _y catalyst treatment		Auger intensity ratios			LEED patterns	
		I _K /I _{Fe}	I _O /I _{Fe}	I _C /I _{Fe}	before	after
(1) EB+H ₂ O	before react.	2.2	3.0	0		
	after react.	1.9	2.8	2.0		
(2) EB+H ₂ O	before react.	0.9	2.3	0.0		
	after react.	0.7	2.7	3.0		
(3) EB+H ₂ O	before react.	4.2	2.8	0	No LEED	No LEED
	after react.	3.1	2.9	1.1		

4.3.2 Carbon formation from dehydrogenation reaction on potassium promoted KFe_xO_y and unpromoted Fe₂O₃ catalysts.

The buildup of carbon deposits was studied by performing the reaction on a promoted catalyst with a $I_K/I_{Fe} = 2.2$ and an unpromoted Fe₂O₃ catalyst. The reaction was interrupted after a few hrs from time on stream and the catalyst was characterized with AES. After that, the reaction was continued. Fig. (4.12) show that the carbon deposits on promoted catalysts increase initially with time on stream but they reach a steady state level which is lower than on the unpromoted Fe₂O₃ catalyst.

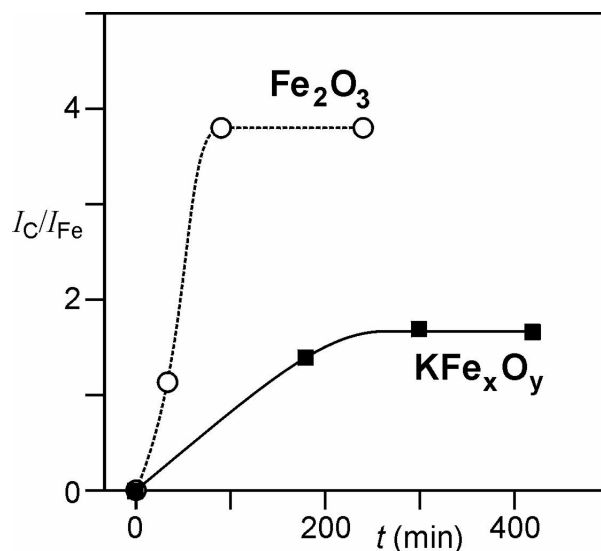


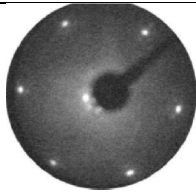
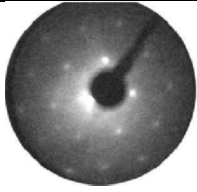
Figure (4.12). The build-up of carbon deposits over the unpromoted Fe_2O_3 and potassium promoted catalyst (KFe_xO_y) expressed by the intensity ratios of the main Auger peaks of carbon to iron (I_C/I_{Fe}) with time on stream.

4.3.3 The effect of steam reactivation on the dehydrogenation reaction over potassium promoted (KFe_xO_y) model catalysts.

Reactivation in industry is done by “steaming”, i.e. by passing only steam over the catalyst. This was simulated in the following way. The reaction was first run for ~4 hrs on a KFe_xO_y model catalyst ($I_K/I_{Fe} = 2.3$). Fig (4.13a) shows the same behavior as seen in Fig (4.10). AES after reaction showed a similar small amount of carbon deposits I_C/I_{Fe} is ~ 0.5 and a moderate loss of potassium (1 in table (4.7)). The reaction was then continued on the catalyst after the EB flow was switched off and the reaction was run for ~ 15 min in presence of water only (reactivation). The EB flow was switched on again and the reaction continued. Fig (4.13b) shows, that the catalyst exhibits a higher starting conversion rate of $\sim 5 \times 10^{15}$ molecules $s^{-1} cm^{-2}$ but the deactivation process is faster now compared to the reaction before reactivation Fig (4.13.a). Characterization by AES after reaction shows a strong increase in the carbon deposits ($I_C/I_{Fe} = 4.4$) and a strong loss of

potassium ($I_K/I_{Fe} = 0.6$), case 2 in table (4.7). The LEED pattern after the reactivation and reaction, has changed to that of Fe_3O_4 which consistent with the strong loss of potassium. The reactivation treatment was repeated on fresh promoted catalyst which this time was characterized before and after the reactivation (Table (4.8)). Here it is obvious It that strong potassium loss occur during this reactivation. In a further experiment, a promoted catalyst covered with carbon deposits was steamed. The treatment effectively removed the carbon deposits.

Table 4.7. LEED patterns and intensity ratios of the main Auger peaks of carbon, oxygen, potassium and iron before and after reaction with EB and H_2O in the feed for the promoted KFe_xO_y model catalysts and effect of reactivation with steam.

KFe _x O _y catalyst treatment		Auger intensity ratios			LEED patterns	
		I_K/I_{Fe}	I_O/I_{Fe}	I_C/I_{Fe}	before	after
(1) EB+H ₂ O	before react.	2.3	2.7	0		No LEED
	after react.	1.8	2.5	0.5		
(2) After react. and 15 min in H ₂ O EB+H ₂ O	before react.	**	**	**	No LEED	
	After react.	0.6	2.6	4.4		

* No AES measurement.

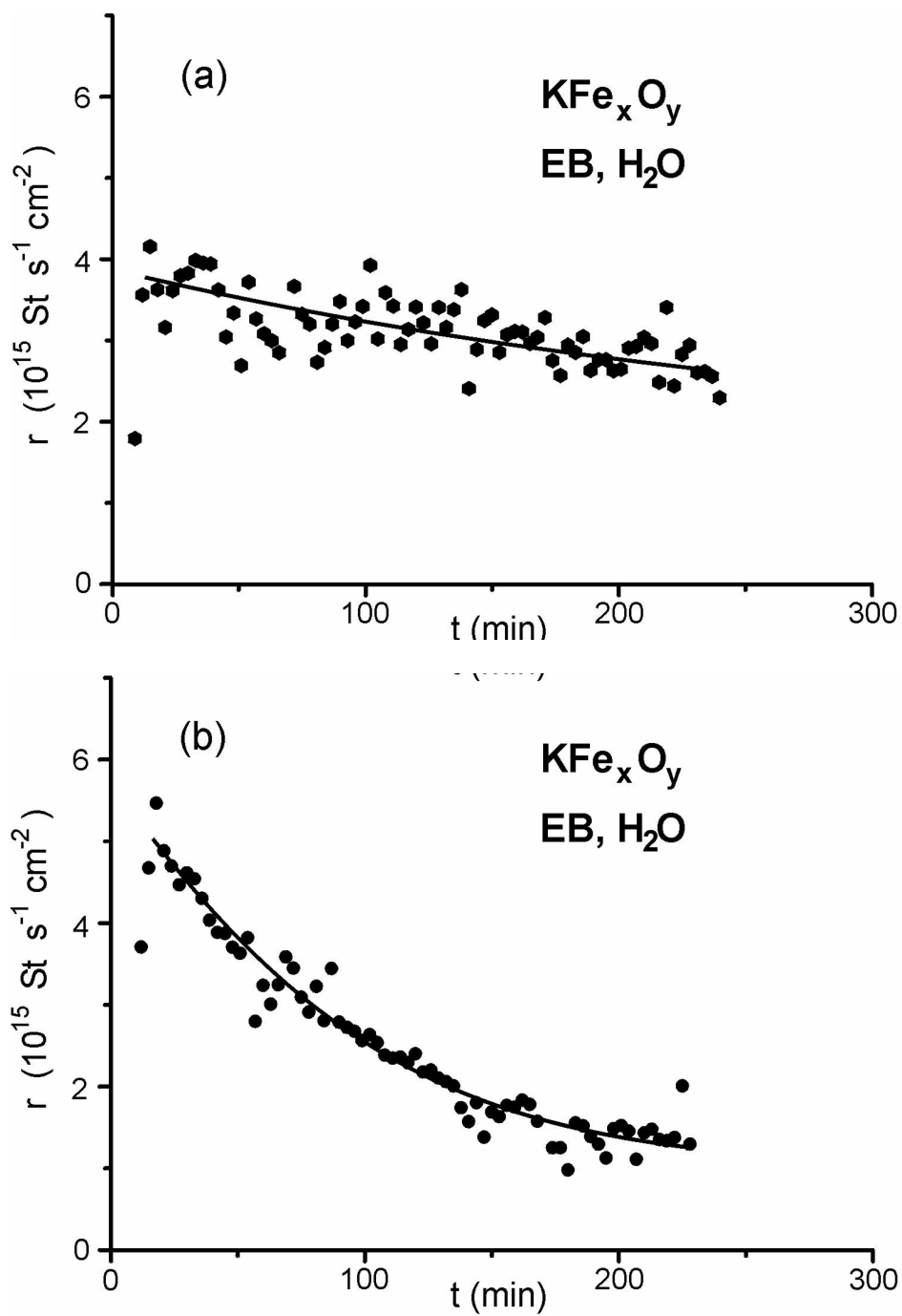
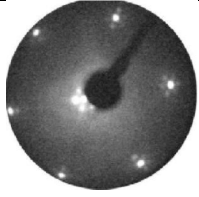


Fig. (4.13). Time dependence of the St conversion rate at 870 K, normal conditions, EB and H_2O in the feed, over KFe_xO_y with $(I_k/I_{Fe} = 2.2)$, a) before reactivation with water, b) after reactivation with water for 15 min.

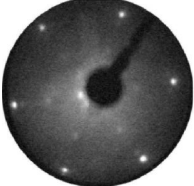
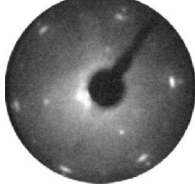
Table 4.8. LEED patterns and intensity ratios of the main Auger peaks of carbon, oxygen, potassium and iron before and after reaction with EB and H₂O in the feed for the promoted KFe_xO_y model catalysts after reactivation with water for 15 min.

KFe _x O _y catalyst treatment		Auger intensity ratios			LEED patterns	
		I _K /I _{Fe}	I _O /I _{Fe}	I _C /I _{Fe}	before	after
EB+H ₂ O	before H ₂ O treatment	2.8	2.7	0.0		No LEED
	after 15 min in H ₂ O	1.2	2.9	0.0		

4.3.4 Dehydrogenation reaction on a potassium promoted KFe_xO_y model catalyst in presence of steam and oxygen.

Here the influence of introducing some oxygen in the feed on the reaction rate and deactivation behavior is studied, on a promoted catalyst (I_K/I_{Fe}=1.0) and compared to the unpromoted Fe₂O₃ catalyst. As Fig. (4.13) shows that oxygen (oxidative conditions table 3.1) in the feed mixture, that the catalyst shows a high conversion rate of $\sim 7 \times 10^{15}$ molecules s⁻¹cm⁻² which is maintained with time on stream and no significant deactivation is seen. The AES measurement after reaction (table (4.9)) shows that the surface is almost free of carbon (I_C/I_{Fe} = 1.0) and the I_O/I_{Fe} ratio is almost unchanged. There is a small loss in the potassium content, LEED shows that the film still exhibits the same (1x1) pattern (i.e. no phase change) but the surface is rougher as concluded from the high background in the LEED image (table (4.9)).

Table 4.9. LEED patterns and intensity ratios of the main Auger peaks of carbon, oxygen, potassium and iron before and after reaction with EB, H₂O and O₂ in the feed (oxidative conditions) for a potassium promoted KFe_xO_y model catalyst ($I_K/I_{Fe} = 1.0$).

KFe _x O _y catalyst treatment		Auger intensity ratios			LEED patterns	
		I _K /I _{Fe}	I _O /I _{Fe}	I _C /I _{Fe}	before	after
EB+H ₂ O +O ₂	before react.	1.0	2.0	0.0		
	after react.	0.9	1.9	0.6		

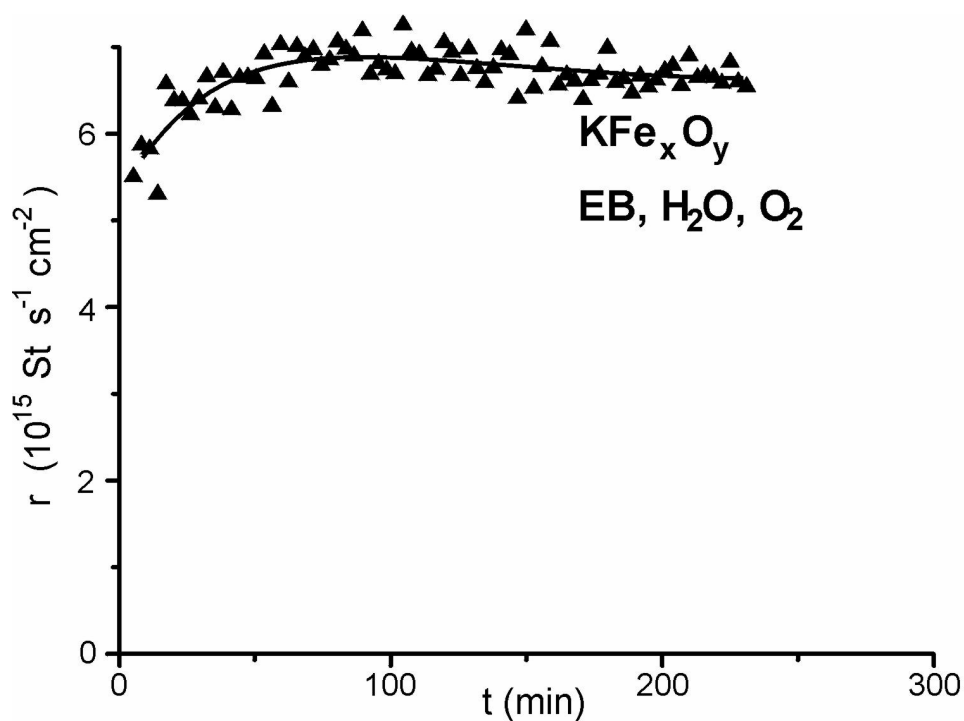


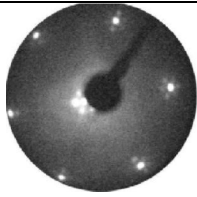
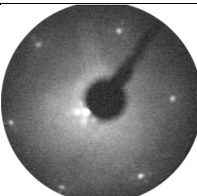
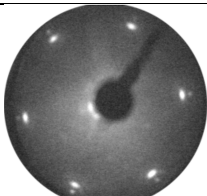
Figure (4.14). Time dependence of the St conversion rate at 870 K, oxidative conditions, EB, H₂O and O₂ in the feed, over KFe_xO_y model catalyst with ($I_K/I_{Fe} = 1.0$).

4.3.5 Dehydrogenation reaction on KFe_xO_y model catalyst without steam, effect of potassium promoting on the reduction of the catalyst.

Here the effect of potassium on the reduction of the promoted catalyst and the role of water in the reaction are studied. The reaction was done on a promoted catalyst with a $\text{I}_\text{K}/\text{I}_\text{Fe}=1.2$ and $\text{I}_\text{O}/\text{I}_\text{Fe}= 2.5$ in absence of steam, only EB with He were introduced. The reaction was interrupted after 45 min. Post reaction characterization with AES showed that the ratio $\text{I}_\text{O}/\text{I}_\text{Fe}$ is almost unchanged (2.5 before and 2.4 after reaction), case 1 in Table (4.9). This indicates that the catalyst is not significantly reduced, in contrast to the unpromoted catalyst which has showed a strong reduction in the absence of water (see F table (4.2)) . This means that potassium stabilizes reduction the promoted catalyst a against reduction.

Fig. (4.15) shows the St conversion rate over a KFe_xO_y catalyst with a $\text{I}_\text{K}/\text{I}_\text{Fe} = 1.9$ with water and EB in the feed (reducing conditions table 3.1). After ~2 hours the water was switched off and replaced by 20 ml of He. There is no sudden decrease in the activity upon switching off of water. This indicates that water is not involved in the rate determining step (RDS) of the reaction. Post reaction characterization with AES showed an increase in the carbon deposits (table 4.10). Comparing the $\text{I}_\text{O}/\text{I}_\text{Fe}$ ratio before and after reaction confirms that there was no strong reduction.

Table(4.10). LEED patterns and intensity ratios of the main Auger peaks of carbon, oxygen, potassium and iron before and after reaction with EB and H₂O or He in the feed over the promoted KFe_xO_y model catalysts.

KFe _x O _y catalyst treatment		Auger intensity ratios			LEED patterns	
		I _K /I _{Fe}	I _O /I _{Fe}	I _C /I _{Fe}	before	after
(1) EB+He	before reaction	1.2	2.4	0.0		No LEED
	after 45 min reaction no	0.9	2.4	0.8		
(2) EB+H ₂ O	before reaction	1.9	2.2	0.0		
	After reaction	1.3	2.0	2.1		

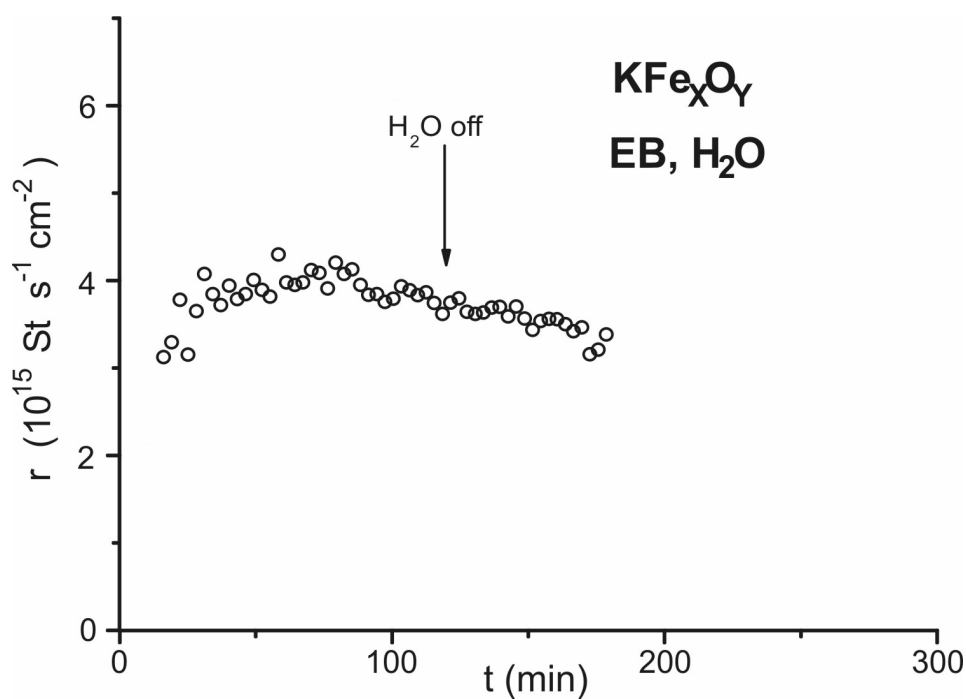


Fig. (4.15). Time dependence of the St conversion rate at 870 K, normal conditions, EB, and H₂O over KFe_xO_y with (I_K/I_{Fe}= 1.9). After 2 hrs H₂O was switched off.

4.3.6 Dehydrogenation reaction on KFe_xO_y (0001) model catalyst in presence of steam and oxygen. Oxygen on and off experiments.

The response of the conversion rate on the oxygen content in the feed was studied in on-off experiments. The switching off of oxygen after ~ 4 hours of reaction on KFe_xO_y ($I_{\text{K}}/I_{\text{Fe}} = 2.7$) under oxidative conditions (table 3.1), showed that the deactivation rate was is very slow. The conversion rate decrease is also slower when compared to the case on the unpromoted catalyst Fig. (4.8a). After 30 min without oxygen, it was switched on a gain and within 20 minutes the initial conversion rate was regained. This shows that oxygen and promotion by potassium play a very similar role and potassium may be replaced by addition of oxygen to the feed.

4.3.7 Dehydrogenation reaction on KFe_xO_y (0001) model catalyst in presence of steam and oxygen. Effect of oxygen concentration.

The effect of decreasing the oxygen concentration added to the feed on the deactivation and St conversion rate for a promoted catalyst ($I_{\text{K}}/I_{\text{Fe}} = 2.7$) is also studied. The oxygen to EB ratio was decreased stepwise after 50 minutes each. Fig. (4.16) shows that decreasing the EB: O_2 ratio to 1:0.3 and to 1: 0.13 does not result in a significant deactivation or decrease in the conversion rate different to the unpromoted catalyst (Fig. (4.7)). The initial rate can be regained after increasing the EB: O_2 ratio again. This indicates also that both oxygen and potassium play a very similar role in preventing the fast deactivation of the catalyst.

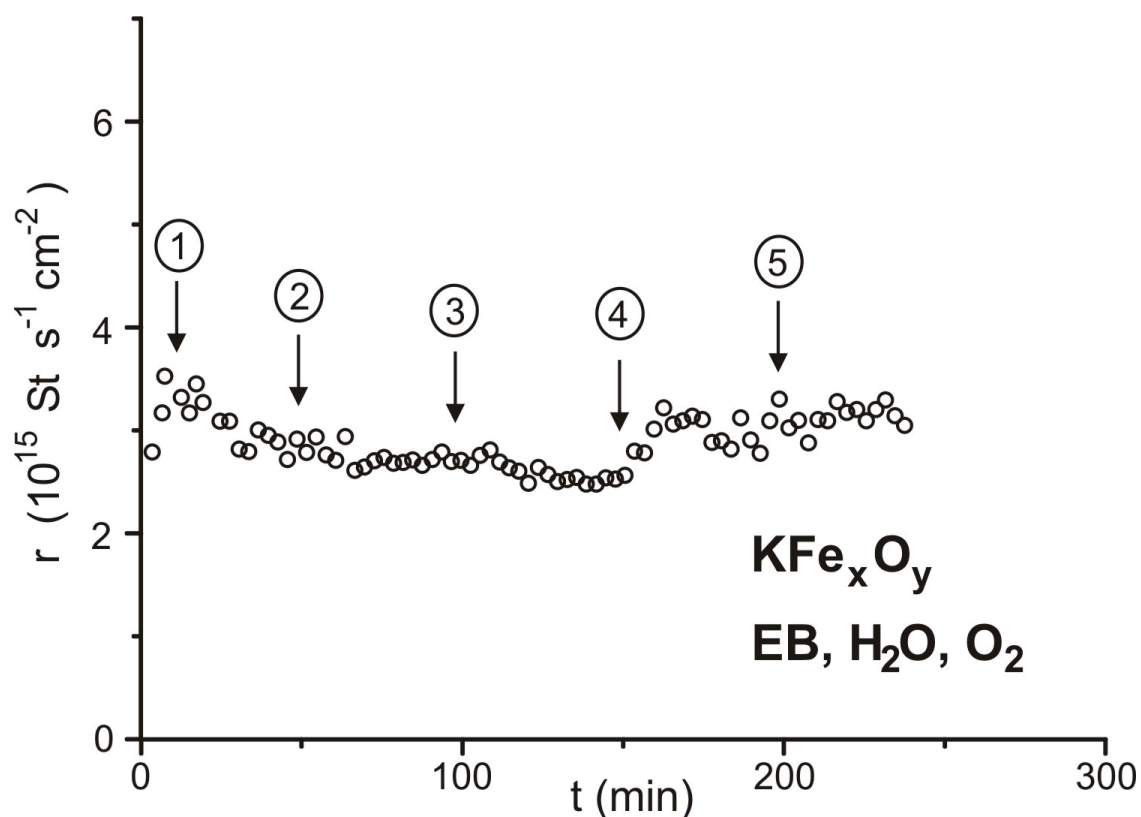


Fig. (4.16). Conversion dependence of the St conversion rate at 870 K, oxidative conditions, EB, H₂O and O₂ in the feed, over KFe_xO_y ($I_K/I_{Fe}=2.7$), on EB/O₂ ratio, (1) 1:0.5, (2) 1:0.3, (3) 1:0.13 (4) 1:0.3 and (5) 1:0.5

4.3.8 Dehydrogenation reaction on $\alpha\text{-Fe}_2\text{O}_3$ (0001) model catalyst in presence of steam and oxygen at different temperature.

Fig.(4.17a) shows the conversion rate of St over a promoted KFe_xO_y model catalyst with a ($I_K/I_{Fe} = 2.8$) in the presence of water and oxygen at different reaction temperatures. As observed on technical catalyst [], the temperature dependence is clear. As in case of unpromoted Fe₂O₃ catalyst, oxygen was added in these experiments in order to keep the catalyst surface clean and prevent deactivation. The resulting from these measurements is presented in more detail in the discussion chapter 5.

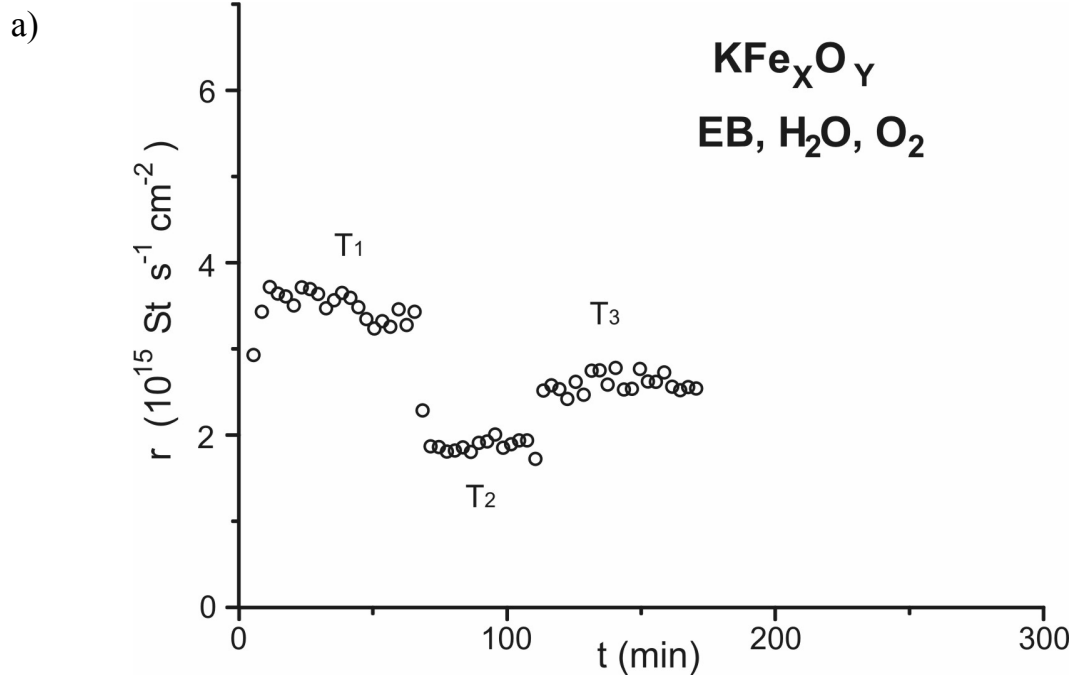


Fig. (4.17). The dependence of the St conversion rate at, normal conditions, EB, H_2O and O_2 in the feed, over a KFe_xO_y ($I_K/I_{Fe}=2.8$) a) at T_1 (894 K), T_2 (846 K) and T_3 (870 k).

4.4 Pressed hematite (Fe_2O_3) powder samples

4.4.1 Reaction on pressed powder pellets in fixed-bed reactor.

In cooperation with G. Kolios and A. Schüle, Institute for chemische Verfahrenstechnik (ICVT), university of Stuttgart, a conversion measurement was performed over pressed pellets of hematite powder in a small fixed bed reactor under the reaction conditions of the technical reaction. The reaction was done with EB and water in the feed (Fig. (4.18) lower curve), and compare them with a measurement where traces of oxygen were added to the feed upper curve. In both cases the reaction rate drops initially, but in the presence of oxygen the rate stabilizes at a value about three times higher than without oxygen. A possible reason could be a stabilization of the hematite phase or burning of coke or both. Switching off the oxygen leads to a quick drop in the rate to the level of the experiment without oxygen. XRD analysis of the spent catalyst shows that it is completely reduced to magnetite, confirming the results observed on the model catalyst.

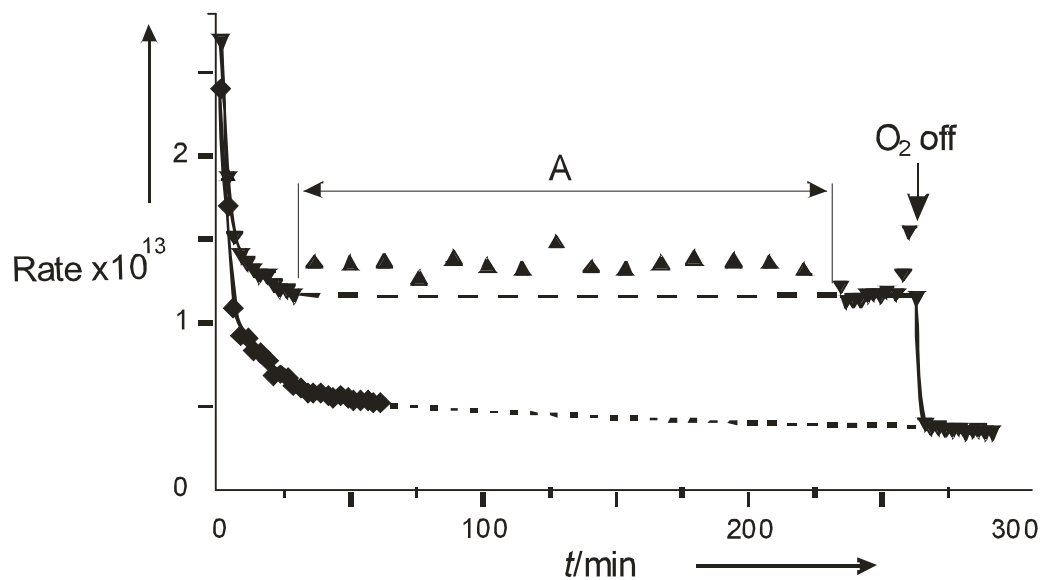


Figure 4.18. Time dependence of the St rate production ($\text{molecules} \cdot \text{s}^{-1} \cdot \text{cm}^{-2}$ BET surface area) over pressed pellets of Fe_2O_3 powder in a fixed bed reactor. Reaction temperature 895 K, atmospheric pressure, $\text{EB}/\text{H}_2\text{O}=1:6$, $\text{EB}/\text{H}_2\text{O}/\text{O}_2=1:6:0.4$. Around point A the GC was switched from fast FID analysis to the combined FID-TCD method, This caused a shift in the baseline.

4.4.2 Reactions on pressed powder pellets in micro-flow reactors.

In addition to the reaction experiments performed on the model catalyst, here we try to study the reaction behavior over pressed hematite powder samples (i.e bulk oxide catalyst) in the micro flow reactor under the same reaction conditions (Table 3.1) used for the model catalysts. Our model catalysts, are thin films of closed surfaces of iron oxide i.e. there is no diffusion limitations or mass and energy transport limitations in contrast to the powder samples. Comparing results from reactions on both type of catalyst will give us an idea if the diffusion and transport limitations on the powder catalyst has an influence on the catalyst performance and this way the pressure and material gap, are bridged. Also try to apply what is seen on the model catalyst i.e. deactivation behavior and stabilization of higher conversion rate with oxygen on the powder catalyst and see if this possible or not.

a. Reaction in the presence of steam and EB in the feed.

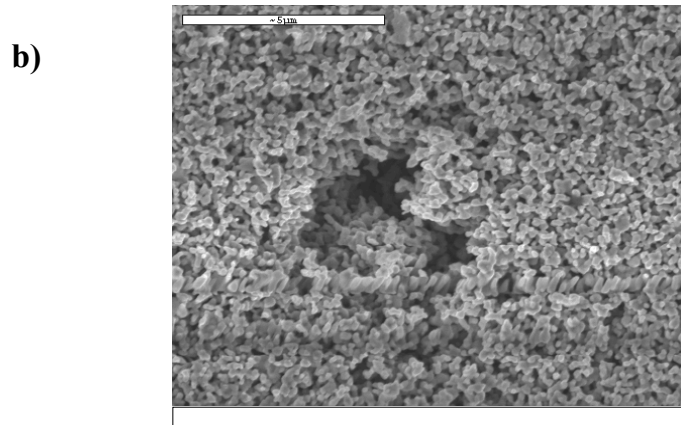
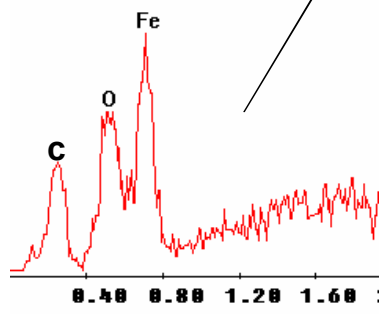
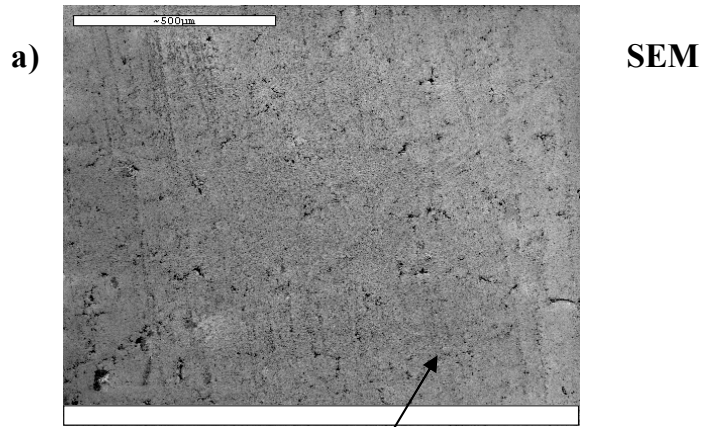
Since hematite is an electrical insulator, the characterization of these pressed powder samples by AES and LEED was not possible because of the charging. Ex-situ characterization methods like SEM-EDX used for characterizing the chemical compositing and particles shape size of these samples before and after reaction.

Fig. (4.19a, b) shows SEM images of the fresh unused sample with different magnification. Fig. (4.19a) with a 5 μm scale show that these samples contain only one type of round particles with size of a bout 0.3 μm . This type of round particles is a result of the grinding and pressing of the powder sample. The SEM image of a higher magnification 2 μm (Fig. (4.19b), shows the particles much more clearly. EDX shows mainly the signals from iron, oxygen and carbon which indicate that the particles consist

of pure iron oxide, but they are not clean. Carbon is mainly concentrated in some areas as shown in Fig (4.19c, d).

The presence of these carbon materials could explain the low activity seen on these samples when they were tested and used without pretreatment in our micro-flow reactor. After 2 cycles of cleaning, (heating for 20 min, in 10^{-1} mbar oxygen at 1000 K), a higher activity of these samples was observed.

The effect of the cleaning pretreatment on the particles shape and size was studied by cleaning a sample by heating for 30 min at 1000 K in 10^{-1} mbar oxygen and then characterizing them using SEM and EDX. In Fig. (4.19e, f). The SEM images shows that there is no significant change in the particle shape or the particle size. EDX shows that the samples are almost free of carbon when compared to the fresh sample. This is in line with the high initial activity after this cleaning procedure Fig. (4.20)).



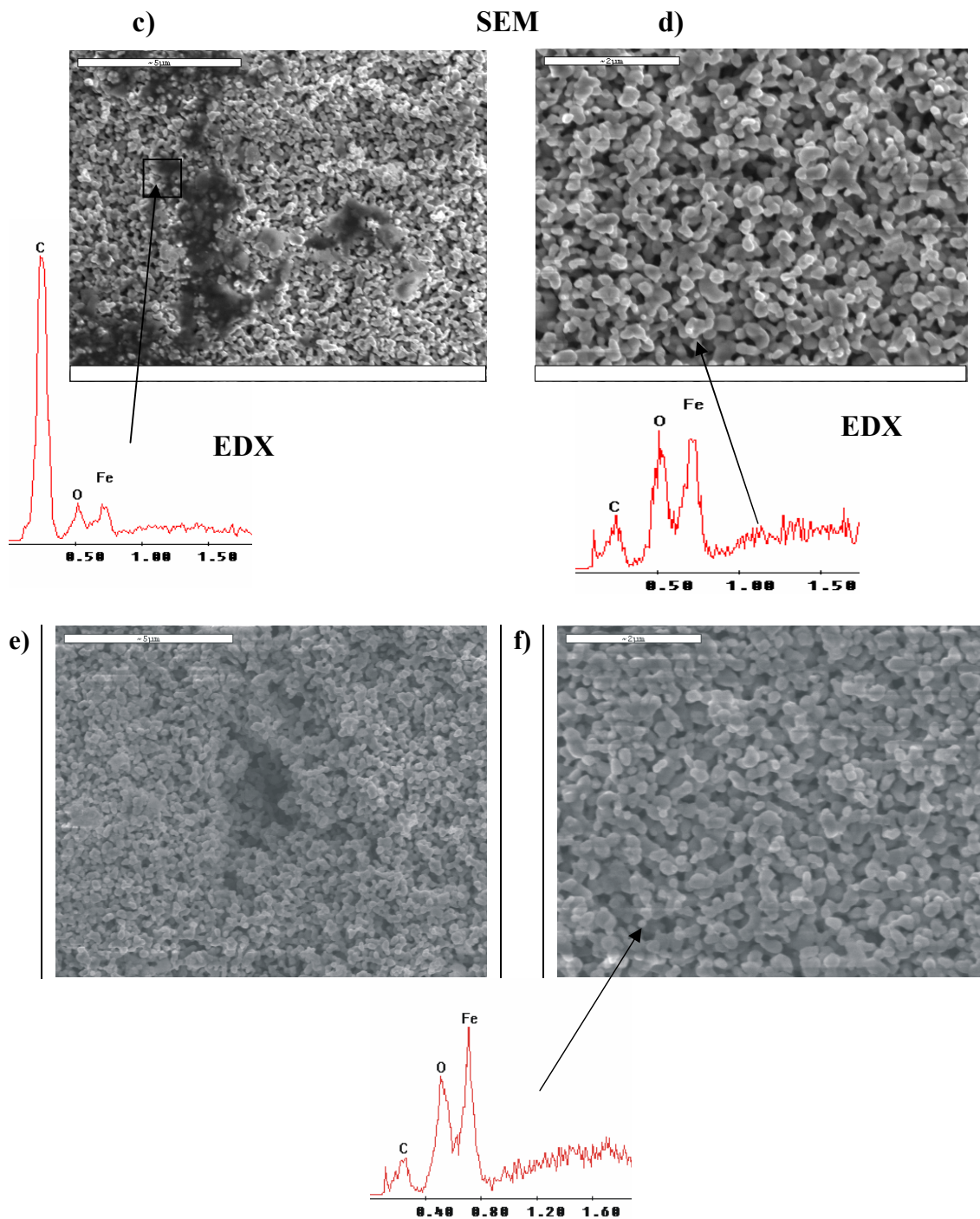


Fig. (4.19). SEM-EDX of the not used sample samples, SEM images with different magnification (a) 500 μm , (b) 5 μm . SEM-EDX unused powder sample showing some carbon covered parts (c) and (d). (e) and (f) SEM-EDX of the sample after cleaning for 30 min in oxygen.

Fig. (4.20a) shows the St conversion over the pressed powder pellet used in the micro flow reactor after cleaning for 30 min at ~ 1025 K in 0.1 mabr oxygen. The reaction was done under non-oxidative conditions (Table 3.1) used for the model catalysts. Different ordinates (at the Y axis) conversion is used here since calculating the conversion rate with respect to the BET surface area ($2.8 \text{ m}^2/\text{g}$) of the powder samples will not scale at all with the conversion rates on the model catalysts. The pressed powder sample show a high starting conversion, then deactivates relatively slowly with time on stream. It is clear that the pressed powder pellet shows a 30 times higher conversion with respect to the geometrical surface area (0.2 cm^2) accessible, when compared to model catalyst. This is may be due to that there is more material i.e. more iron oxide active sites. However, since conversion does not scale with the BET area, this indicates the most of the pores are not accessible or show only slow gas exchange. The deactivation rate is relatively slower compared to the model catalyst.

After reaction the sample was taken out of the reactor for post reaction characterization. The sample surface was red (i.e. still Fe_2O_3) and the back was black. The sample was broken into tow halves, which showed that the sample is also black from inside and the red area is only a very thin layer on the surface. Part of the sample was grounded for characterization with XRD, which shows that the sample is reduced to magnetite (Fe_3O_4) as shown in Fig. (4.20b).

Characterization with SEM-EDX the ungrounded part of the sample, shows that the red layer on the surface was very thin, and the rest of the sample was black. The difference between Fe_2O_3 and Fe_3O_4 in quantification with SEM-EDX, is too little to get a valuable

results to differentiate between them at the interface between the red and black layers as shown in Fig. (4.21a, b). The SEM images show also that there is a mixture of particles with different sizes like the one in the fresh sample Fig. (4.21b), and others are smaller particles $\sim 0.1 \mu m$ size are formed and this maybe due to the breaking of the particles by the degradation process which occur by the reduction of the Fe_2O_3 to Fe_3O_4 under the reaction conditions, the images are shown with tow different magnification as shown in (Fig. 4.22a, b). Also EDX shows that they are covered by some carbon deposits Fig. (4.22b).

There were also carbon deposits on the surface of these particles forming carbon clusters . Fig. (4.23). The sensitivity of the SEM can not tell us if the particles are covered completely by a closed thin films of carbon or they are just in form of islands as shown in Fig. (4.24a, b) which shows different SEM images with different magnification. Fig (4.24 c, d) show a larger magnification of the carbon clusters formed on the particle surface.

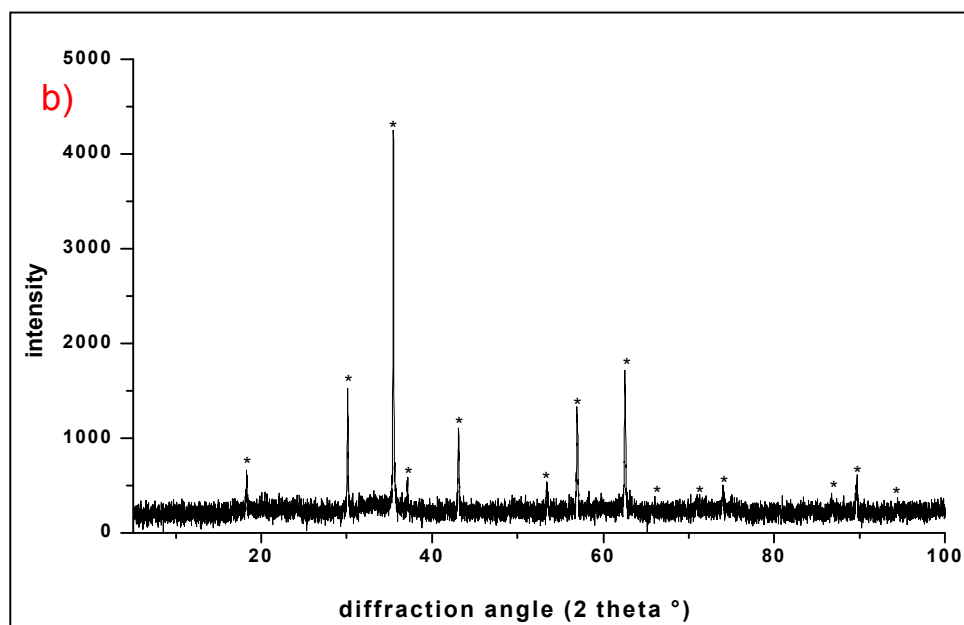
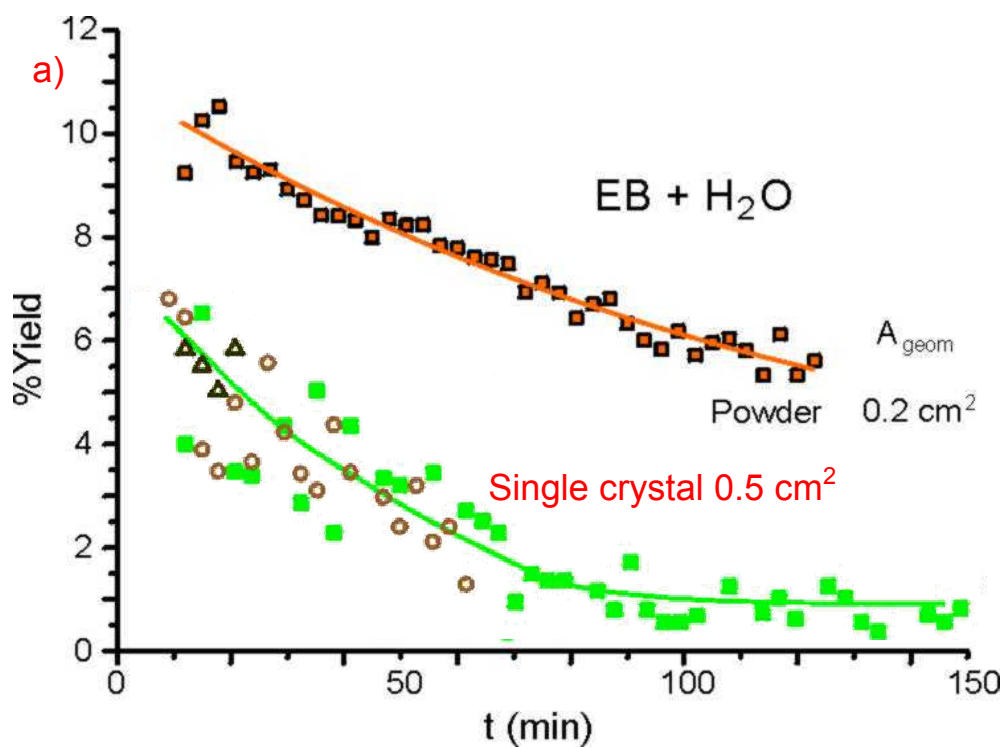


Fig. (4.20). a) St yield over the pressed powder Fe_2O_3 pellets used in the micro-flow reactor at the same conditions like the model catalyst of 870 K and EB and water in the feed. b) XRD spectrum of the powder sample after reaction.

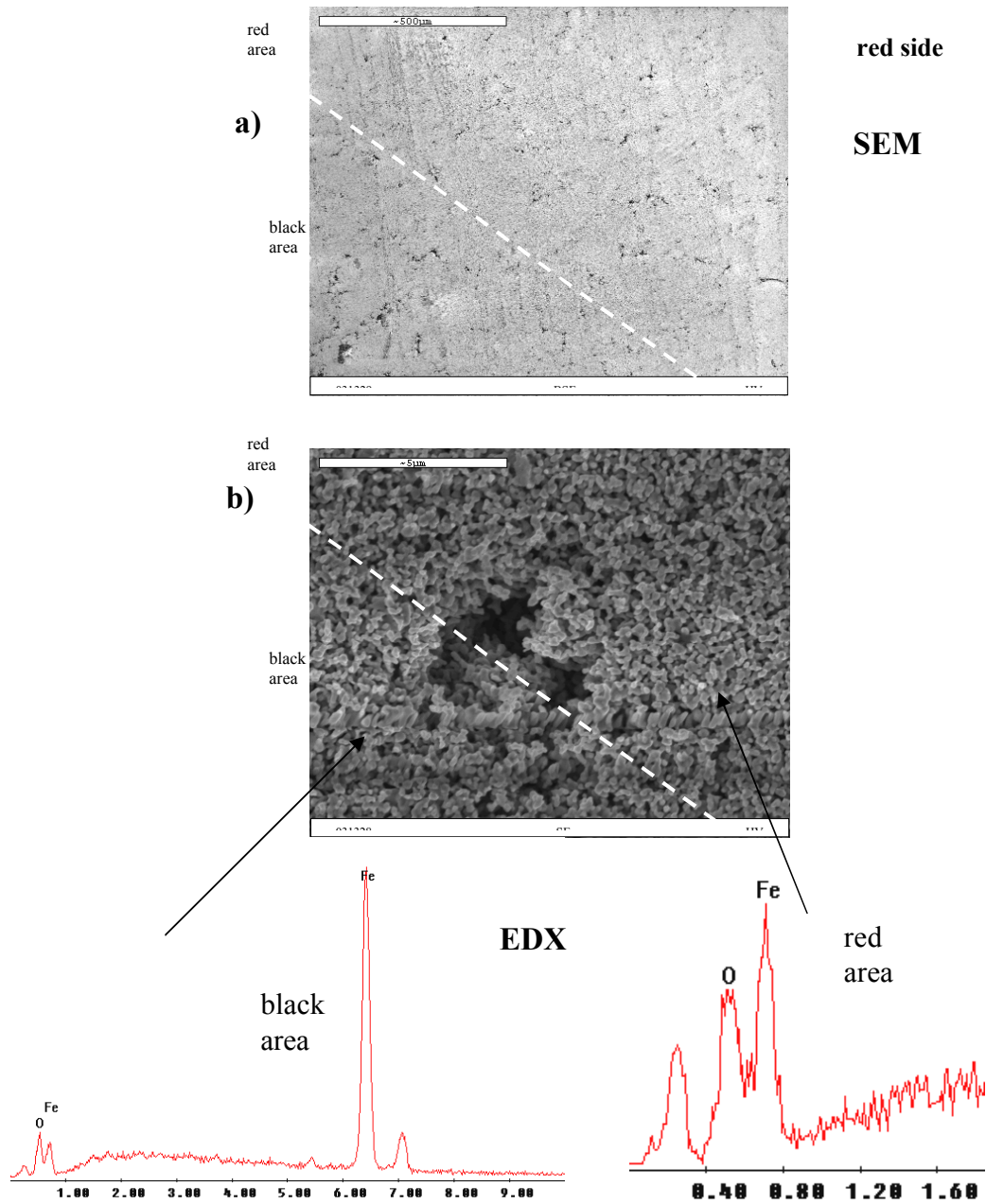


Fig. (4.21). SEM and EDX of the powder sample after reaction with EB and H₂O in the feed with different magnification a) 500 μm, b) 5 μm.. Only the surface of the sample was red (Fe₂O₃) and the bulk was black (Fe₃O₄). It was not possible to differentiate between the both phases and no material difference is seen.

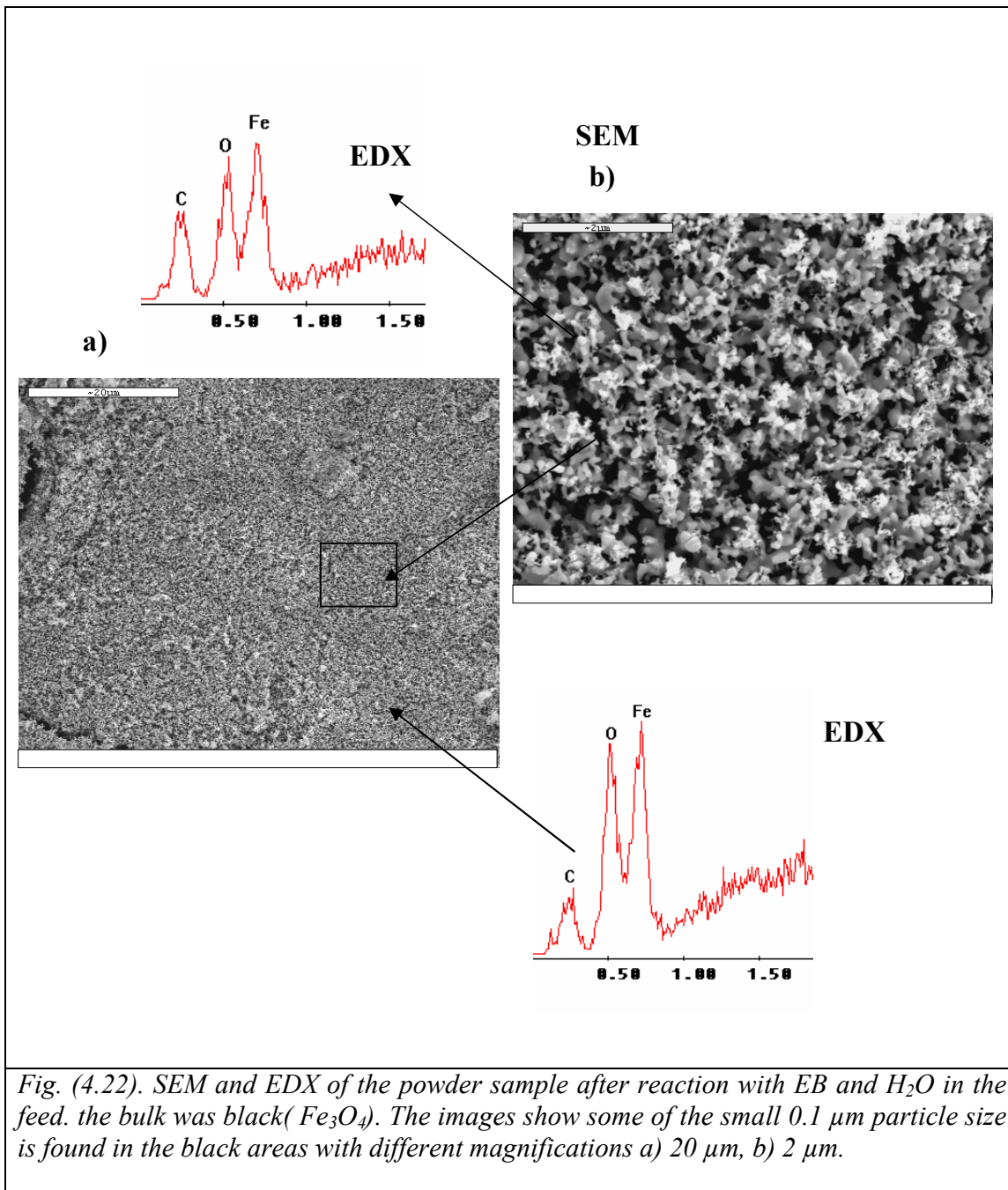


Fig. (4.22). SEM and EDX of the powder sample after reaction with EB and H₂O in the feed. the bulk was black(Fe₃O₄). The images show some of the small 0.1 μm particle size is found in the black areas with different magnifications a) 20 μm, b) 2 μm.

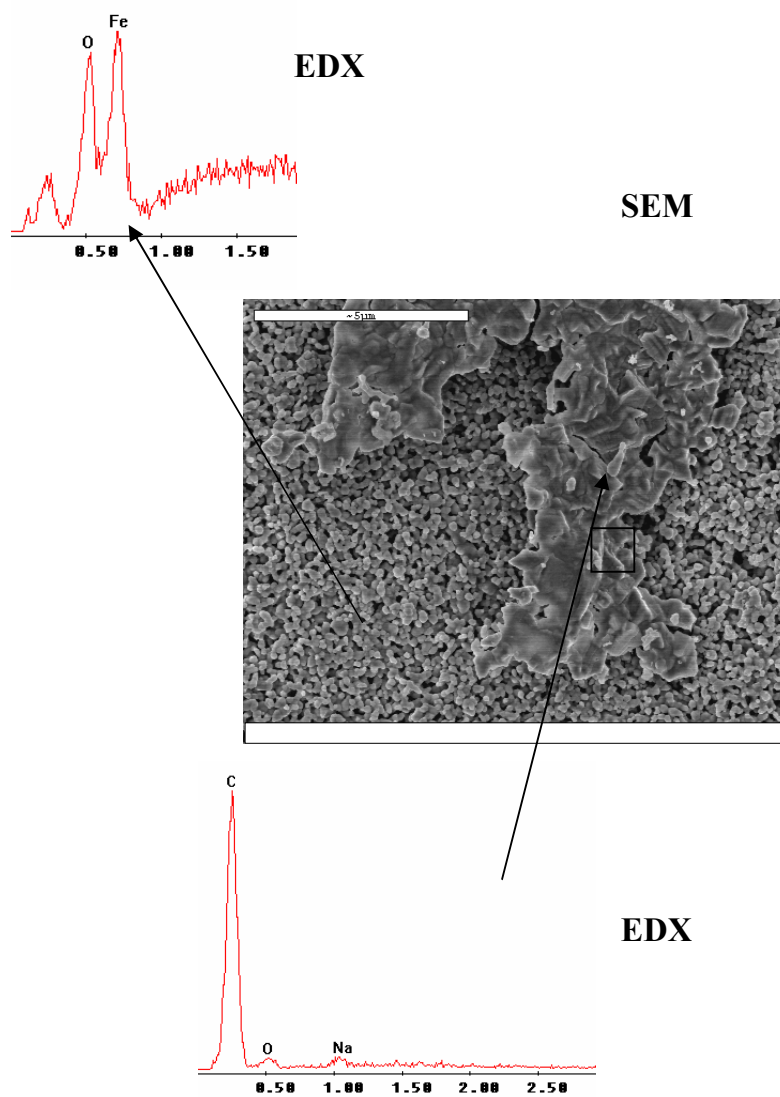


Fig. (4.22). SEM and EDX of the powder sample after reaction with EB and H₂O in the feed. Only the surface of the sample was red (Fe₂O₃) and the bulk was black (Fe₃O₄). The carbon deposits are quite clear seen here.

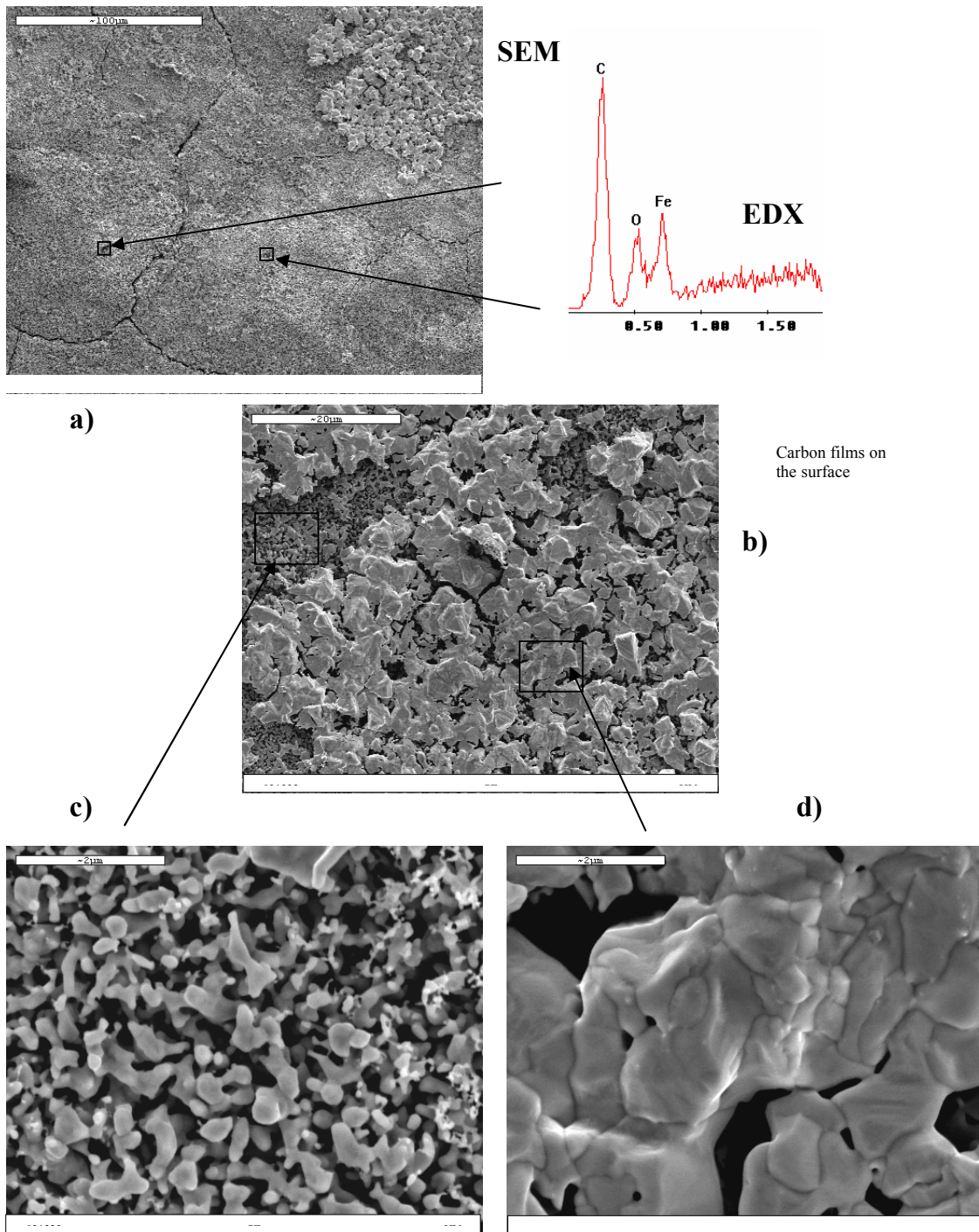


Fig. (4.23). SEM and EDX of the powder sample after reaction with EB and H₂O in the feed. The black side and parts of the sample (Fe₃O₄). A carbon film on the surface is seen in the lower right image.

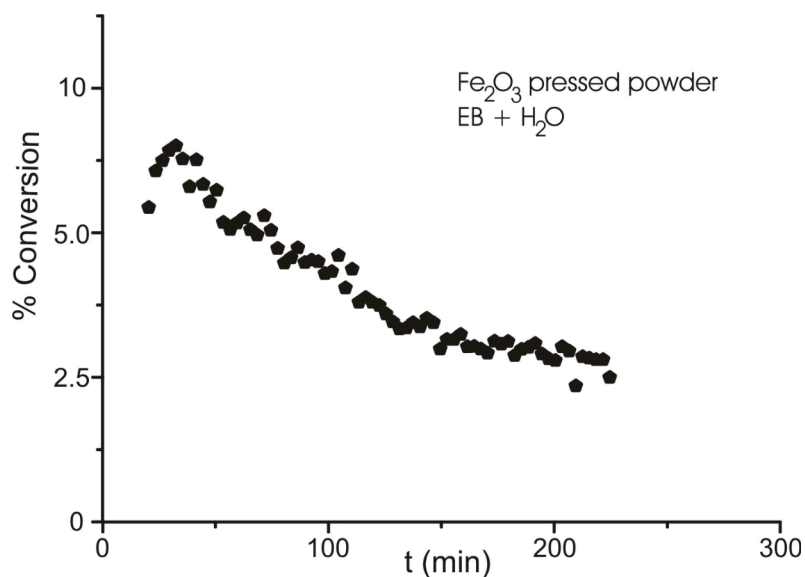
b) Reaction in the presence of EB, water and oxygen in the feed.

Fig. (4.25a) show the St conversion over the powder sample under non oxidative conditions (Table 3.1) on a new sample. The catalyst shows a high starting conversion but it deactivates relatively slowly with time on stream. This shows that the experiments are reproducible and show the same behavior as in Fig. (4.21) After 4 hrs on stream, the reaction was stopped and the sample was taken out of the reactor. The sample was completely black and it was found to be magnetic (Fe_3O_4) using a rough test with a permanent magnet as explained in the experimental chapter. The sample was returned back to the reactor and it was reoxidized using same conditions used in the cleaning procedure of the fresh samples. The reaction was continued on the sample but with the presence of oxygen in the feed (oxidative conditions table 3.1). Fig. (4.26b) shows the styrene conversion is high and the activity of the catalyst is almost constant with slower deactivation rate with time on stream. So admitting oxygen led to the stabilization of a higher yield as seen on the model catalyst. After reaction the sample was taken out from the reactor the sample was completely red with some grey-black spots at the back of the sample.

The sample was characterized using XRD and SEM-EDX. The XRD shows that the sample is still mainly hematite, i.e. the reduction to magnetite (Fe_3O_4) was prevented, which agrees with the results shown on the model catalyst. The SEM-EDX analysis shows that there are tow types of particles, round ones like in the fresh sample Fig. (4.26), Fig. (4.27a, b, C and D) and a plain rectangular particles up to 1 μm in length and width and these particles are not only on the surface but they are also below the surface .This is maybe due to re-crystallization of the particles due to the reduction and

reoxidation of the Fe_2O_3 to Fe_3O_4 and the back to Fe_2O_3 . At the back of the sample where the grey-black spots were seen, two types of particles are seen one like the fresh sample and other ones with a bigger size up to $2\ \mu\text{m}$ Fig. (4.28).

(a)



(b)

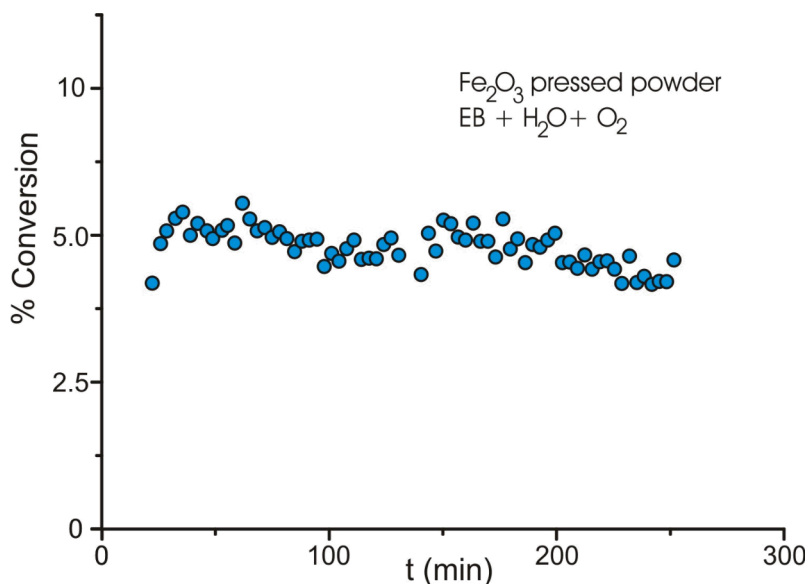


Fig. (4.25). a) *St* yield over the pressed powder Fe_2O_3 pellets used in the micro-flow reactor at the same conditions like the model catalyst of 870 K and EB and water in the feed. B) in the presence of oxygen in the feed.

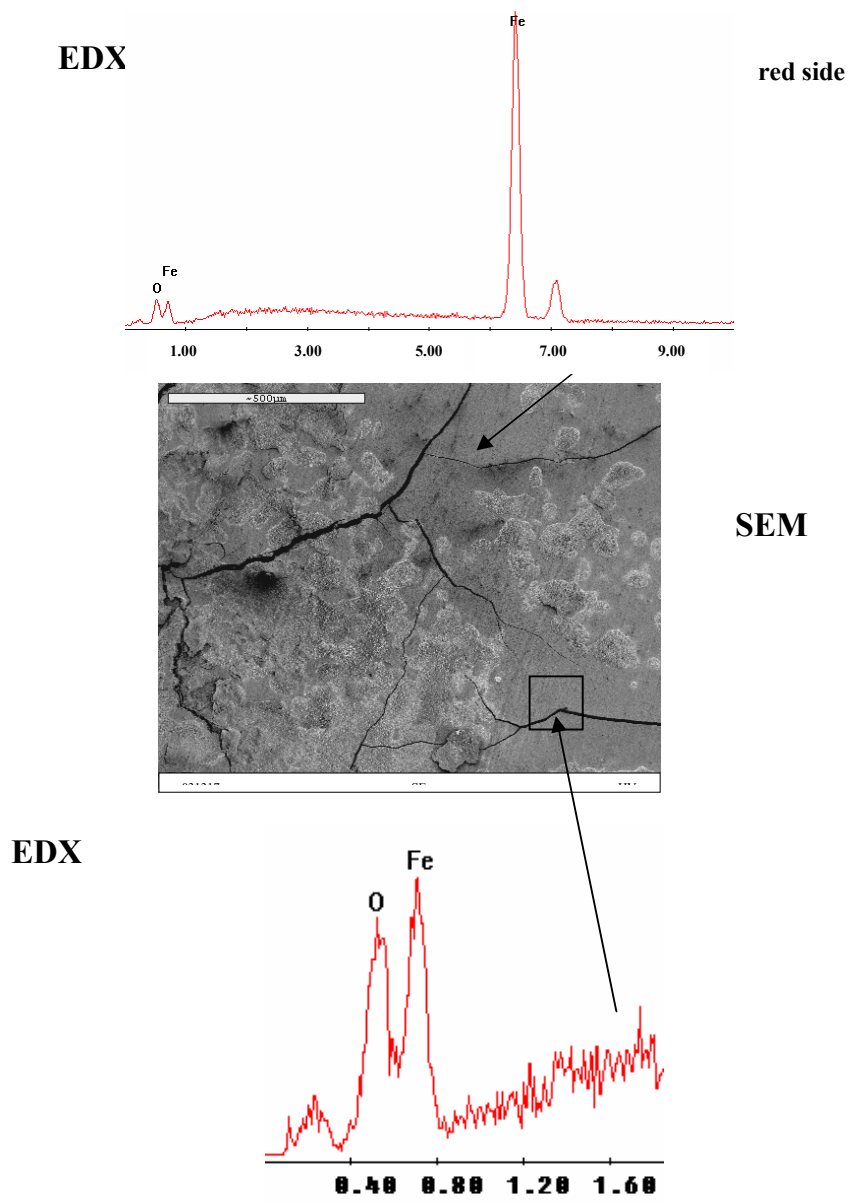


Fig. (4.26). SEM and EDX of the powder sample after reaction with EB and H₂O in the feed. the sample was red (Fe₂O₃) and the EDX analysis shows that the surface is almost clean from the carbon deposits.

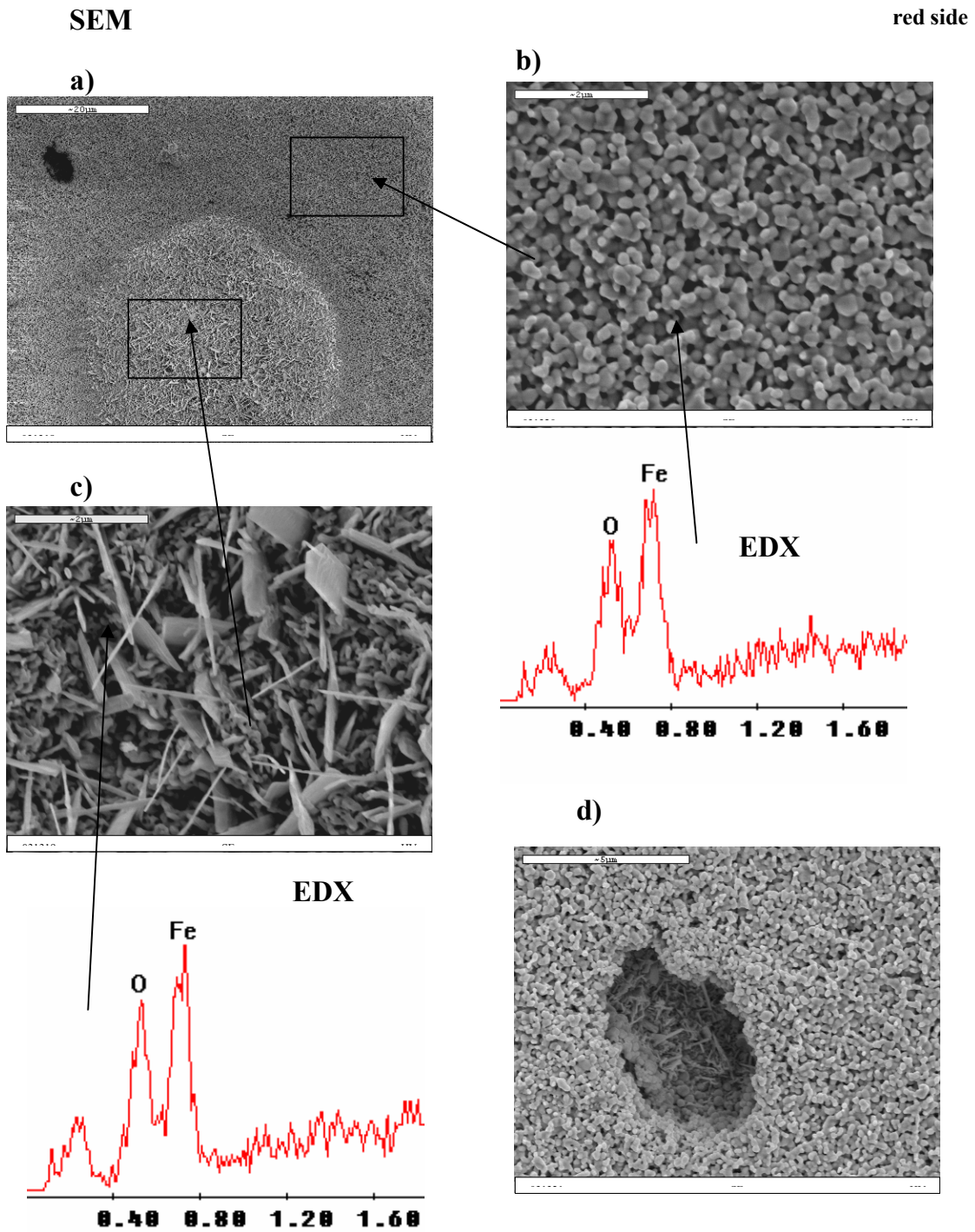


Fig. (4.27). SEM and EDX of the powder sample after reaction with EB and H₂O in the feed. the sample was red (Fe₂O₃) SEM shows that big particle with a 1µm in size are formed on the surface and in the bulk.

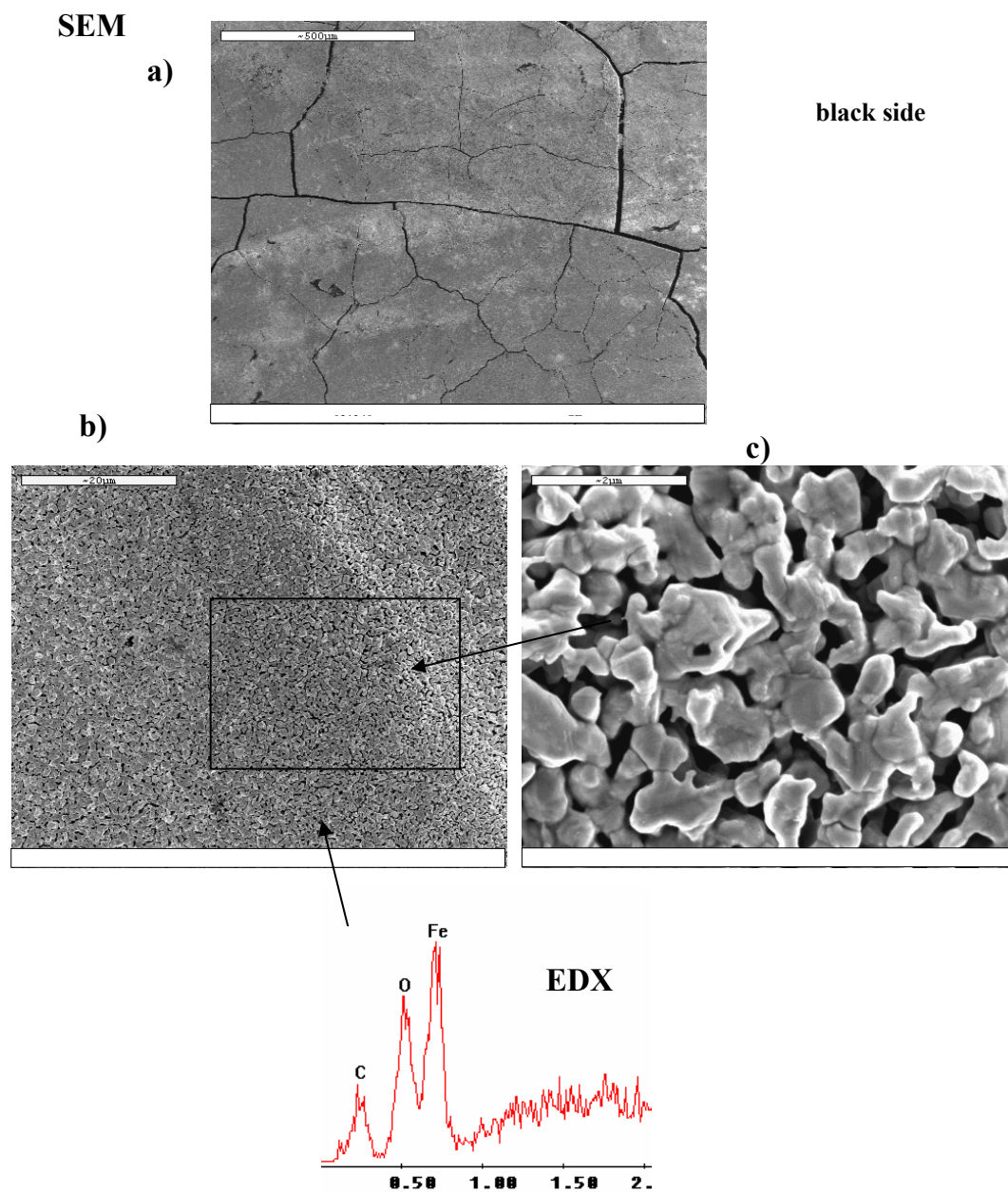


Fig. (4.28). SEM and EDX of the powder sample after reaction with EB and H₂O in the feed. the surface of the sample was red (Fe₂O₃) and the back was black. SEM images show different particles with bigger particle size and EDX show some carbon deposits